

Dimeric *n*-Alkyl Complexes of Rare-Earth Metals Supported by a Linked Amido–Cyclopentadienyl Ligand: Evidence for β -Agostic Bonding in Bridging *n*-Alkyl Ligands and Its Role in Styrene Polymerization

Peter Voth, Stefan Arndt, Thomas P. Spaniol, and Jun Okuda*

Institut für Anorganische Chemie und Analytische Chemie, Johannes Gutenberg-Universität Mainz, Duesbergweg 10-14, D-55099 Mainz, Germany

Lily J. Ackerman

Department of Chemistry, California Institute of Technology, Pasadena, California 91125

Malcolm L. H. Green

Inorganic Chemistry Laboratory, Oxford University, South Parks Road, Oxford OX1 3QR, United Kingdom

Received August 13, 2002

The dimeric rare-earth hydrides $[\text{Ln}(\eta^5\text{:}\eta^1\text{-C}_5\text{Me}_4\text{SiMe}_2\text{NCMe}_3)(\text{THF})(\mu\text{-H})_2]$ ($\text{Ln} = \text{Y, Yb}$) react with excess α -olefin $\text{H}_2\text{C}=\text{CHR}$ ($\text{R} = \text{Et, } ^n\text{Pr, } ^n\text{Bu}$) in a 1,2-insertion to give the series of THF-free dimeric *n*-alkyl complexes $[\text{Ln}(\eta^5\text{:}\eta^1\text{-C}_5\text{Me}_4\text{SiMe}_2\text{NCMe}_3)(\mu\text{-CH}_2\text{CH}_2\text{R})_2]$ as isolable crystals. Single-crystal X-ray diffraction studies on the five derivatives $[\text{Y}(\eta^5\text{:}\eta^1\text{-C}_5\text{Me}_4\text{SiMe}_2\text{NCMe}_2\text{R}')(\mu\text{-CH}_2\text{CH}_2\text{R})_2]$ ($\text{R}' = \text{Me, R} = \text{Et, } ^n\text{Bu; R}' = \text{Et, R} = \text{Et, } ^n\text{Pr}$) and $[\text{Yb}(\eta^5\text{:}\eta^1\text{-C}_5\text{Me}_4\text{SiMe}_2\text{NCMe}_3)(\mu\text{-CH}_2\text{CH}_2^n\text{Bu})_2]$ revealed that the centrosymmetric dimeric complexes consist of two trans-arranged $[\text{Ln}(\eta^5\text{:}\eta^1\text{-C}_5\text{Me}_4\text{SiMe}_2\text{NCMe}_2\text{R}')]_2$ fragments connected by two μ -alkyl ligands. Most strikingly, there is an agostic interaction of the *n*-alkyl groups' β -CH₂ hydrogen atoms with the formally 12-electron lanthanide metal center. Variable-temperature NMR spectroscopic data suggest a fluxional process that interconverts the diastereotopic protons of the α -CH₂ group and a dynamic β -agostic interaction. Addition of >10 equiv of THF per yttrium to a solution of $[\text{Y}(\eta^5\text{:}\eta^1\text{-C}_5\text{Me}_4\text{SiMe}_2\text{NCMe}_3)(\mu\text{-CH}_2\text{CH}_2\text{Et})_2]$ results in the formation of the highly reactive, nonisolable, monomeric THF adduct $[\text{Y}(\eta^5\text{:}\eta^1\text{-C}_5\text{Me}_4\text{SiMe}_2\text{NCMe}_3)(\text{CH}_2\text{CH}_2\text{Et})(\text{THF})]$. Reaction of 1,2-dimethoxyethane (DME) with $[\text{Y}(\eta^5\text{:}\eta^1\text{-C}_5\text{Me}_4\text{SiMe}_2\text{NCMe}_3)(\mu\text{-CH}_2\text{CH}_2\text{Et})_2]$ forms the crystalline compound $[\text{Y}(\eta^5\text{:}\eta^1\text{-C}_5\text{Me}_4\text{SiMe}_2\text{NCMe}_3)(\text{CH}_2\text{CH}_2\text{Et})(\text{DME})]$ with a terminal *n*-butyl group that contains a slightly distorted α -carbon atom according to a crystallographic study. α -Olefins having two or more substituents on the γ -carbon do not react with the hydride complexes. The role of these *n*-alkyl complexes in the controlled polymerization of styrene is discussed.

Introduction

In catalytic reactions such as hydrogenation and various hydrometalations of α -olefins, the insertion of the α -olefin into the metal–hydride bond within the coordination sphere of a group 3 metallocene is one of the most fundamental steps.¹ The resulting alkyl, however, further inserts α -olefins only sluggishly, and other types of reactions such as β -hydride elimination, β -alkyl elimination, and σ -bond metathesis commonly prevail.² Living α -olefin polymerization by lanthanocene catalysts therefore remains difficult to achieve.^{3–8} Bercaw et al. reported⁹ that the scandium hydrido complex $[\text{Sc}(\eta^5\text{:}\eta^1\text{-C}_5\text{Me}_4\text{SiMe}_2\text{NCMe}_3)(\text{PMe}_3)(\mu\text{-H})_2]$, containing

a sterically open linked amido–cyclopentadienyl ligand,¹⁰ repeatedly inserts α -olefins (in a 1,2-fashion), establishing the first example of a quasi-living α -olefin oligomerization by a well-defined organo rare-earth metal complex. The insertion products are isolable either as the PMe_3 adduct $[\text{Sc}(\eta^5\text{:}\eta^1\text{-C}_5\text{Me}_4\text{SiMe}_2\text{NCMe}_3)\text{R}(\text{PMe}_3)]$ (R

(1) (a) Watson, P. L.; Parshall, G. *Acc. Chem. Res.* **1985**, *18*, 51. (b) Schaverien, C. J. *Adv. Organomet. Chem.* **1994**, *36*, 283. (c) Edelmann, F. T. In *Comprehensive Organometallic Chemistry II*; Abel, E. W., Stone, F. G. A., Wilkinson, G., Eds.; Pergamon Press: Oxford, U.K., 1995; Vol. 4, p 11. (d) Chirik, P. J.; Bercaw, J. E. *Metallocenes*; Halterman, R. L., Togni, A., Eds.; Wiley-VCH: Weinheim, Germany, 1998; p 111.

(2) (a) Watson, P. L. *J. Am. Chem. Soc.* **1983**, *105*, 6491. (b) Baxter, S. M.; Bulls, A. R.; Burger, B. J.; Nolan, B. D.; Santarsiero, W.; Schaefer, W. P.; Bercaw, J. E. *J. Am. Chem. Soc.* **1987**, *109*, 203. (c) Burger, B. J.; Thompson, M. E.; Cotter, W. D.; Bercaw, J. E. *J. Am. Chem. Soc.* **1990**, *112*, 1566.

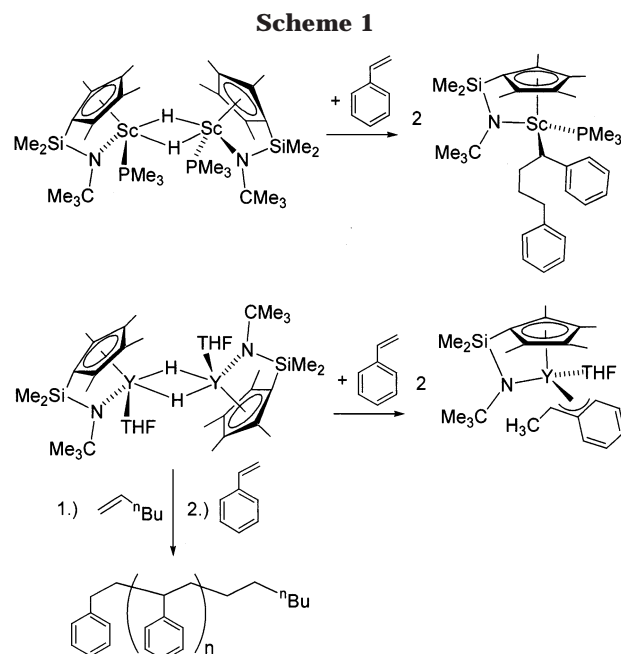
(3) Examples of living α -olefin polymerization: Doi, Y.; Keii, T. *Adv. Polym. Sci.* **1986**, *73/74*, 201. Doi, Y.; Tokuhira, N.; Soga, K. *Makromol. Chem., Macromol. Chem. Phys.* **1989**, *190*, 643.

(4) Hagihara, H.; Shiono, T.; Ikeda, T. *Macromolecules* **1998**, *31*, 3184. Hasan, T.; Ioku, A.; Nishii, K.; Shiono, T.; Ikeda, T. *Macromolecules* **2001**, *34*, 3142. Fukui, Y.; Murata, M.; Soga, K. *Macromol. Rapid. Commun.* **1999**, *20*, 637.

(5) Scollard, J. D.; McConville, D. H. *J. Am. Chem. Soc.* **1996**, *118*, 1008. Baumann, R.; Davis, W. M.; Schrock, R. R. *J. Am. Chem. Soc.* **1997**, *119*, 3830. Liang, L. C.; Schrock, R. R.; Davis, W. M.; McConville, D. H. *J. Am. Chem. Soc.* **1999**, *121*, 5797. Mehrkhodavandi, P.; Schrock, R. R. *J. Am. Chem. Soc.* **2001**, *123*, 10746.

= alkyl) or as the dimer $[\text{Sc}(\eta^5\text{-}\eta^1\text{-C}_5\text{Me}_4\text{SiMe}_2\text{NCMe}_3)(\mu\text{-R})_2]$, featuring two-electron–three-center bonds. On the basis of detailed equilibrium and kinetic studies, the active species was concluded to be the 12-electron species $[\text{Sc}(\eta^5\text{-}\eta^1\text{-C}_5\text{Me}_4\text{SiMe}_2\text{NCMe}_3)\text{R}]$.^{9c}

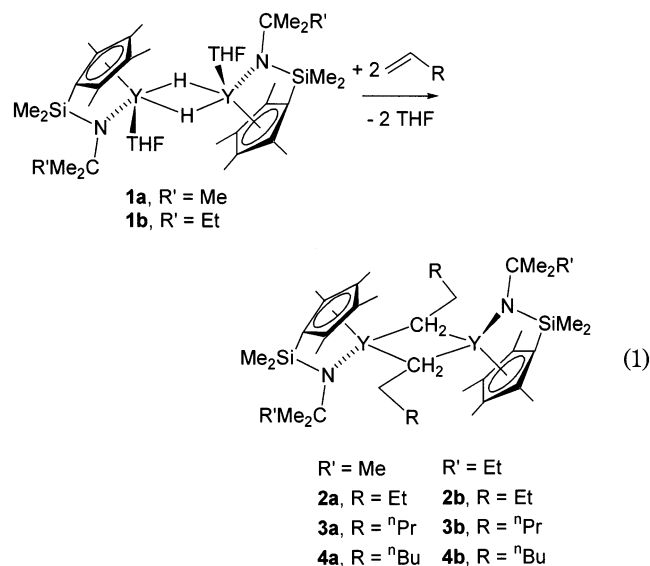
In the context of developing structurally well-defined organometallic initiators for controlled styrene polymerization,^{11,12} we have been studying the homologous complexes of the larger rare-earth metals and recently reported the synthesis and characterization of hydrido complexes of the type $[\text{Ln}(\eta^5\text{-}\eta^1\text{-C}_5\text{Me}_4\text{SiMe}_2\text{NCMe}_3)(\text{THF})(\mu\text{-H})_2]$ ($\text{Ln} = \text{Y, Lu, Yb}$).¹³ Whereas the scandium hydrido complex $[\text{Sc}(\eta^5\text{-}\eta^1\text{-C}_5\text{Me}_4\text{SiMe}_2\text{NCMe}_3)(\text{PMe}_3)(\mu\text{-H})_2]$ was found to give a product of double insertion, $[\text{Sc}(\eta^5\text{-}\eta^1\text{-C}_5\text{Me}_4\text{SiMe}_2\text{NCMe}_3)\{\text{CH}(\text{Ph})\text{CH}_2\text{CH}_2\text{CH}_2\text{Ph}\}(\text{THF})]$,^{9c} the yttrium hydrido complex was shown to react with styrene to give a stable monoinsertion product, $[\text{Y}(\eta^5\text{-}\eta^1\text{-C}_5\text{Me}_4\text{SiMe}_2\text{NCMe}_3)\{\text{CH}(\text{Ph})\text{CH}_3\}(\text{THF})]$ (Scheme 1).^{13b} Neither complex initiates styrene polymerization. Styrene can be polymerized, however, when the dimeric yttrium hydride $[\text{Y}(\eta^5\text{-}\eta^1\text{-C}_5\text{Me}_4\text{SiMe}_2\text{NCMe}_3)(\text{THF})(\mu\text{-H})_2]$ is first reacted with 1-hexene to give what we initially believed to be the monoinsertion product $[\text{Y}(\eta^5\text{-}\eta^1\text{-C}_5\text{Me}_4\text{SiMe}_2\text{NCMe}_3)(\text{CH}_2\text{CH}_2\text{C}_6\text{H}_5)(\text{THF})_n]$, possibly with a dinuclear structure ($x = 2$). To gain further insight into this activation procedure, we have isolated



a series of alkyl complexes resulting from the monoinsertion of 1-alkene into the lanthanide–hydride bond. We describe here details of their structure and their role in styrene polymerization.

Results and Discussion

Insertion of α -Olefins. When the yttrium hydrides $[\text{Y}(\eta^5\text{-}\eta^1\text{-C}_5\text{Me}_4\text{SiMe}_2\text{NCMe}_2\text{R})(\text{THF})(\mu\text{-H})_2]$ ($\text{R}' = \text{Me}$ (**1a**), Et (**1b**)) were treated in benzene or toluene with a large excess of α -olefin $\text{H}_2\text{C}=\text{CHR}$ ($\text{R} = \text{Et}$, ^nPr , ^nBu) at room temperature, the THF-free monoinsertion products $[\text{Y}(\eta^5\text{-}\eta^1\text{-C}_5\text{Me}_4\text{SiMe}_2\text{NCMe}_2\text{R})(\mu\text{-CH}_2\text{CH}_2\text{R})_2]$ ($\text{R}' = \text{Me}$, $\text{R} = \text{Et}$ (**2a**), ^nPr (**3a**), ^nBu (**4a**); $\text{R}' = \text{Et}$, $\text{R} = \text{Et}$ (**2b**), ^nPr (**3b**), ^nBu (**4b**)) form according to eq 1. All the



monoinsertion products could be isolated as extremely air- and moisture-sensitive colorless crystals in good yields (40–60%). For successful isolation, it is crucial to keep the concentration of α -olefin high. The crystals are soluble in aromatic hydrocarbons and less so in aliphatic hydrocarbons and are best recrystallized from

(6) Saito, J.; Mitani, M.; Mohri, J.; Ishii, S.; Yoshida, Y.; Matsugi, T.; Kojoh, S. H.; Kashiwa, N.; Fujita, T. *Chem. Lett.* **2001**, 576. Kojoh, S.; Matsugi, T.; Saito, J.; Mitani, M.; Fujita, T.; Kashiwa, N. *Chem. Lett.* **2001**, 822. Saito, J.; Mitani, M.; Onda, M.; Mohri, J.; Ishii, S.; Yoshida, Y.; Nakano, T.; Tanaka, H.; Matsugi, T.; Kojoh, S. H.; Kashiwa, N.; Fujita, T. *Macromol. Rapid Commun.* **2001**, 22, 1072. Tian, J.; Hustad, P. D.; Coates, G. W. *J. Am. Chem. Soc.* **2001**, 123, 5134. Tshuva, E. Y.; Goldberg, I.; Kol, M. *J. Am. Chem. Soc.* **2000**, 122, 10706. Tshuva, E. Y.; Goldberg, I.; Kol, M.; Goldschmidt, Z. *Inorg. Chem. Commun.* **2000**, 3, 611.

(7) Jayaratne, K. C.; Sita, L. R. *J. Am. Chem. Soc.* **2000**, 122, 958. Jayaratne, K. C.; Keaton, R. J.; Henningsen, D. A.; Sita, L. R. *J. Am. Chem. Soc.* **2000**, 122, 10490. Keaton, R. J.; Jayaratne, K. C.; Henningsen, D. A.; Koterwas, L. A.; Sita, L. R. *J. Am. Chem. Soc.* **2001**, 123, 10754.

(8) Killian, C. M.; Tempel, D. J.; Johnson, L. K.; Brookhart, M. *J. Am. Chem. Soc.* **1996**, 118, 11664.

(9) (a) Shapiro, P. J.; Bunel, E. E.; Schaefer, W. P.; Bercaw, J. E. *Organometallics* **1990**, 9, 867. (b) Piers, W. E.; Shapiro, P. J.; Bunel, E. E.; Bercaw, J. E. *Synlett* **1990**, 74. (c) Shapiro, P. J.; Cotter, W. D.; Schaefer, W. P.; Labinger, J. A.; Bercaw, J. E. *J. Am. Chem. Soc.* **1994**, 116, 4623.

(10) (a) McKnight, A. L.; Waymouth, R. M. *Chem. Rev.* **1998**, 98, 2587. (b) Okuda, J.; Eberle, T. *Metalloenes*; Halterman, R. L., Togni, A., Eds.; Wiley-VCH: Weinheim, Germany, 1998; p 415.

(11) Syndiospecific styrene polymerization: (a) Ishihara, N.; Semimiya, T.; Kuramoto, M.; Uoi, M. *Macromolecules* **1986**, 19, 2464. (b) Ishihara, N.; Kuramoto, M.; Uoi, M. *Macromolecules* **1988**, 21, 3356. (c) Pellecchia, C.; Longo, P.; Grassi, A.; Ammendola, P.; Zambelli, A. *Macromol. Rapid Commun.* **1987**, 8, 277. (d) Oliva, L.; Pellecchia, C.; Cinquina, P.; Zambelli, A. *Macromolecules* **1989**, 22, 1642. (e) Zambelli, A.; Oliva, L.; Pellecchia, C. *Macromolecules* **1989**, 22, 2129. (f) Pellecchia, C.; Longo, P.; Proto, A.; Zambelli, A. *Macromol. Rapid Commun.* **1992**, 13, 265. (g) Grassi, A.; Lambert, C.; Zambelli, A.; Mingozzi, I. *Macromolecules* **1997**, 30, 1884. (h) Quyoum, R.; Wang, Q.; Tudoret, M.-J.; Baird, M. C. *J. Am. Chem. Soc.* **1994**, 116, 6435. (i) Pellecchia, C.; Pappalardo, D.; Oliva, L.; Zambelli, A. *J. Am. Chem. Soc.* **1995**, 117, 6593.

(12) (a) Harder, S.; Feil, F.; Knoll, K. *Angew. Chem., Int. Ed.* **2001**, 40, 4261. (b) Harder, S.; Feil, F. *Organometallics* **2002**, 21, 2268. (c) Tanaka, K.; Furo, M.; Ihara, E.; Yasuda, H. *J. Polym. Sci., Part A: Polym. Chem.* **2001**, 39, 1382.

(13) (a) Hultzsich, K. C.; Spaniol, T. P.; Okuda, J. *Angew. Chem., Int. Ed.* **1999**, 38, 227. (b) Hultzsich, K. C.; Voth, P.; Beckerle, K.; Spaniol, T. P.; Okuda, J. *Organometallics* **2000**, 19, 228. (c) Arndt, S.; Voth, P.; Spaniol, T. P.; Okuda, J. *Organometallics* **2000**, 19, 4690. (d) Okuda, J.; Arndt, S.; Beckerle, K.; Hultzsich, K. C.; Voth, P.; Spaniol, T. P. *Pure Appl. Chem.* **2001**, 73, 351. (e) Okuda, J.; Arndt, S.; Beckerle, K.; Hultzsich, K. C.; Voth, P.; Spaniol, T. P. In *Organometallic Catalysts and Olefin Polymerization*; Blom, R., Follestad, A., Rytter, E., Tilset, M., Ystenes, M., Eds.; Springer: Berlin, 2001; p 156. (f) Trifonov, A. A.; Spaniol, T. P.; Okuda, J. *Organometallics* **2001**, 20, 4869.

Table 1. Experimental Data for the Crystal Structure Determinations of the *n*-Butyl Complexes **2a and **9a****

	2a	9a
Crystal Data		
empirical formula	C ₃₈ H ₇₂ N ₂ Si ₂ Y ₂	C ₂₃ H ₄₆ NO ₂ SiY
fw	791.00	485.62
cryst color	colorless	colorless
cryst size, mm	0.35 × 0.32 × 0.12	0.18 × 0.08 × 0.07
cryst system	monoclinic	monoclinic
space group	<i>P</i> 2 ₁ / <i>n</i> (No. 14)	<i>P</i> 2/ <i>c</i> (No. 13)
<i>a</i> , Å	11.3212(8)	20.173(1)
<i>b</i> , Å	13.961(1)	8.9298(8)
<i>c</i> , Å	13.906(1)	15.431(2)
α, deg	90	90
β, deg	106.492(1)	109.005(2)
γ, deg	90	90
<i>V</i> , Å ³	2107.5(3)	2628.2(4)
<i>Z</i>	4/2	4
ρ _{calcd} , g cm ⁻³	1.246	1.227
μ, mm ⁻¹	2.822	2.281
<i>F</i> (000)	840	1040
Data Collection		
2θ _{max} , deg	57	57
index ranges		
<i>h</i>	−15 to 15	−26 to 26
<i>k</i>	−18 to 18	−11 to 11
<i>l</i>	−18 to 18	−20 to 20
Solution and Refinement		
no. of rflns measd	18 930	23 687
no. of indep rflns	5219 (<i>R</i> _{int} = 0.031)	6497 (<i>R</i> _{int} = 0.140)
no. of obsd rflns	4054 (<i>I</i> > 2σ(<i>I</i>))	2904 (<i>I</i> > 2σ(<i>I</i>))
no. of params	389	427
GOF	0.960	0.877
final <i>R</i> indices <i>R</i> ₁ , w <i>R</i> ₂		
obsd data	0.0257/0.0559	0.0513/0.0874
all data	0.0399/0.0581	0.1609/0.1163
<i>e</i> (max)/ <i>e</i> (min), e Å ⁻³	0.480/−0.282	0.450/−0.635

toluene solutions at −30 °C. They gradually decompose even under argon at room temperature over a period of days. Whereas the lutetium complex reacted only sluggishly with α-olefins, the trivalent ytterbium hydride [Yb(η⁵:η¹-C₅Me₄SiMe₂NCMe₃)(THF)(μ-H)]₂ (**5a**)^{13c} afforded with 1-hexene dark red crystals of the monoinsertion product [Yb(η⁵:η¹-C₅Me₄SiMe₂NCMe₃)(μ-CH₂-CH₂ⁿBu)]₂ (**6a**). α-Olefins with two or more substituents on the γ-carbon did not react with the hydride complexes.

Crystal Structures. Crystals of the five complexes **2a**, **2b**, **3b**, **4a**, and **6a**, suitable for X-ray diffraction studies, were obtained by slow cooling of toluene or benzene/hexane solutions. Crystallographic data for the representative derivative **2a** are listed in Table 1, and those for the other four complexes are compiled in Table 3. Figure 1 shows the ORTEP diagram of **2a**. The ORTEP diagrams of the other four complexes can be found in the Supporting Information. Pertinent bond distances and bond angles of all five complexes are listed in Table 2, as are those of the homologous scandium complex [Sc(η⁵:η¹-C₅Me₄SiMe₂NCMe₃)(μ-CH₂CH₂CH₃)]₂ reported previously.^{9c} All five complexes are dimeric with trans-disposed ancillary ligands, exhibiting crystallographically imposed *C*₂ symmetry. The differences in the geometrical parameters, including those of the linked amido-cyclopentadienyl ligand between the scandium, yttrium, and ytterbium derivatives, can be ascribed to their differing ionic radii.¹⁴

The two *n*-alkyl ligands bridge the two metal fragments to form a distorted square, reminiscent of struc-

tures of dimeric aluminum trialkyls Al₂R₆,¹⁵ as well as dimeric lanthanocene dialkyls such as [(η⁵-C₅H₅)₂Yb(μ-Me)]₂^{16a} and heterobimetallic complexes such as [(η⁵-C₅H₅)₂Ln(μ-Me)₂AlMe₂]₂^{16b} and [(η⁵-C₅H₅)₂Ln(μ-Me)₂Li(TMEDA)]₂.^{16c,17} In **2a**, the distances between yttrium and the bridging α-carbon atoms are practically identical at 2.542(2) and 2.544(2) Å, and the angles at these carbon atoms are 88.14(6)°. The yttrium–yttrium distance was found to be 3.5370(4) Å, shorter than the value of 3.672(1) Å found in the dimeric hydride **1a**.^{13a}

The most notable feature of the crystal structures is the conformation of the β-CH₂ groups that accommodate the “fifth” coordination site at the yttrium center with a square-pyramidal geometry. As expected from the overall *C*₂ symmetry of the molecule, the amido groups are not in the plane dissecting the Ln₂C₂ core. Rather, they are bent away from the metal–metal axis, opening space in one lateral sector of the coordination sphere. Although not all of the hydrogen atoms of the LnCH₂-CH₂ portions could be determined due to disorder, the acute angle at the C_α atom Ln–C_α–C_β (84.7(5)° in **2a**) as well as the short distance between the β-carbon atom and the metal center (2.83(1) Å) all hint at the presence of β-agostic bonding. In the low-temperature structure of **2a**, both β-hydrogen atoms could be located, despite some disorder. One of them clearly points to the yttrium center, characterized by the angles C_β–H–Y = 107° and H–Y–C_α = 49°. Thus, it is apparent that one of the CH bonds of the β-carbon atom completes the square-pyramidal configuration of the four-legged piano stool.

For the hydrogen at the bridging α-carbon, refinements converged with positions in agreement with a trigonal-bipyramidal carbon center. The alkyl chain and the opposite yttrium atom adopt the apical positions with Y–C16′–C17′ = 165.3(4)°, whereas the yttrium atom and the two hydrogen atoms define the equatorial plane. The five-coordinate carbon atoms of the bridging methyl groups generally tend to adopt a distorted-trigonal-bipyramidal configuration, as has been reported for [Y(η⁵-C₅Me₄SiMe₃){(μ-Me)AlMe₂(μ-OCMe₃)}]₂,¹⁸ [Nd-(AlMe₄)₃(Al₂Me₆)_{0.5}],¹⁹ and [Sm(OC₆H₃Me₂-2,6){(μ-Me)-AlMe₂}]₂.²⁰ To our knowledge, the only other structure with a bridging higher alkyl group in a dinuclear rare-earth complex was reported by Marks et al. for the μ-ethyl dilutetium complex [(Et₂Si(η⁵-C₅H₄)(η⁵-C₅Me₄)-Lu]₂(μ-H)(μ-Et), for which a β-agostic interaction was

(14) Shannon, R. D. *Acta Crystallogr., Sect. A* **1976**, *32*, 751. For coordination number 8, Sc = 0.870 Å, Y = 1.019 Å, and Yb = 0.985 Å; for coordination number 6, Sc = 0.745 Å, Y = 0.900 Å, and Yb = 0.868 Å.

(15) McGrady, G. S.; Turner, J. F. C.; Ibberson, R. M.; Prager, M. *Organometallics* **2000**, *19*, 4398.

(16) (a) Holton, J.; Lappert, M. F.; Ballard, D. G. H.; Pearce, R.; Atwood, J. L.; Hunter, W. E. *J. Chem. Soc., Dalton Trans.* **1979**, 54. (b) Holton, J.; Lappert, M. F.; Ballard, D. G. H.; Pearce, R.; Atwood, J. L.; Hunter, W. E. *J. Chem. Soc., Dalton Trans.* **1979**, 45. (c) Schumann, H.; Lauke, H.; Hahn, E.; Heeg, M. J.; Van der Helm, D. *Organometallics* **1985**, *4*, 321. (d) Evans, W. J.; Drummond, D. K.; Hanusa, T. P.; Doedens, R. J. *Organometallics* **1987**, *6*, 2279. (e) Shen, Q.; Cheng, Y.; Lin, Y. *J. Organomet. Chem.* **1991**, *419*, 293.

(17) For a recent review on lanthanide alkyls, see: Cotton, S. A. *Coord. Chem. Rev.* **1997**, *160*, 93.

(18) Evans, W. J.; Boyle, T. J.; Ziller, J. W. *J. Organomet. Chem.* **1993**, *462*, 141.

(19) Klooster, W. T.; Lu, R. S.; Anwander, R.; Evans, W. J.; Koetzle, T. F.; Bau, R. *Angew. Chem., Int. Ed.* **1998**, *37*, 1268.

(20) Gordon, J. C.; Giesbrecht, G. R.; Brady, J. T.; Clark, D. L.; Keogh, D. W.; Scott, B. L.; Watkin, J. G. *Organometallics* **2002**, *21*, 127.

Table 2. Selected Bond Distances (Å) and Angles (deg) for Complexes of the Type [Ln(η^5 - η^1 -C₅Me₄SiMe₂NCMe₂R')(μ -CH₂CH₂R)]₂ (2a, 2b, 3b, 4a, and 6a) as well as the *n*-Propyl Scandium Complex [Sc(η^5 - η^1 -C₅Me₄SiMe₂NCMe₃)(μ -CH₂CH₂CH₃)₂]^{9c}

	Ln					Sc
	Y (2a)	Y (2b)	Y (3b)	Y (4a)	Yb (6a)	
R	Et	Et	Substituents			
R'	Me	Et	ⁿ Pr	ⁿ Bu	ⁿ Bu	Me
			Et	Me	Me	Me
			Bond Distances			
Ln-C _α	2.542(2)	2.52(1)	2.519(6)	2.499(6)	2.460(5)	2.334(7)
Ln-C _{α'}	2.544(2)	2.56(1)	2.535(6)	2.522(6)	2.470(5)	2.372(7)
Ln...Ln	3.5370(4)	3.546(2)	3.5318(8)	3.5350(9)	3.449(2)	3.310(2)
Ln-C _β	2.82(1)/2.85(1)	2.83(1)	2.801(6)	2.82(1)/2.90(1)	2.83(2)/2.84(2)	2.913
C _α -C _β	1.49(1)/1.53(1)	1.47(2)	1.456(8)	1.48(1)/1.49(1)	1.44(2)/1.51(1)	1.47(1)
			Bond Angles			
Ln-C _α -Ln'	88.14(6)	88.4(5)	88.7(2)	89.5(2)	88.8(2)	95.7(5)
Ln-C _α -C _β	147.5(3)/165.3(4)	154(1)	168.3(5)	156.9(8)/174.9(6)	149.8(7)/173.0(8)	144.0(5)
C _α -C _β -C _γ	125(1)/117.0(9)	116(1)	125.6(6)	117.4(9)/121.1(9)	121(1)/127(1)	117.5(7)
C _α -Ln-C _{α'}	91.86(6)	91.6(5)	91.3(2)	90.5(2)	91.2(2)	90.6(2)

Table 3. Experimental Data for the Crystal Structure Determinations of the Complexes 2b, 3b, 4a, and 6a

	2b	3b	4a	6a
	Crystal Data			
formula	C ₄₀ H ₇₆ N ₂ Si ₂ Y ₂	C ₄₂ H ₈₀ N ₂ Si ₂ Y ₂	C ₄₂ H ₈₀ N ₂ Si ₂ Y ₂	C ₄₂ H ₈₀ N ₂ Si ₂ Yb ₂
fw	819.02	847.08	847.10	1015.34
cryst color	colorless	colorless	colorless	red
cryst size, mm	0.58 × 0.50 × 0.30	0.85 × 0.73 × 0.50	0.43 × 0.42 × 0.28	0.86 × 0.72 × 0.38
cryst syst	monoclinic	monoclinic	triclinic	triclinic
space group	<i>P</i> 2 ₁ / <i>n</i> (No. 14)	<i>P</i> 2 ₁ / <i>n</i> (No. 14)	<i>P</i> 1 (No. 2)	<i>P</i> 1 (No. 2)
<i>a</i> , Å	12.967(2)	11.4118(7)	10.1087(8)	10.153(5)
<i>b</i> , Å	13.388(2)	15.122(2)	10.5126(6)	10.471(4)
<i>c</i> , Å	13.850(2)	14.182(1)	10.6309(8)	11.514(8)
α, deg	90	90	101.686(5)	101.10(4)
β, deg	110.70(1)	109.795(7)	101.380(6)	101.88(5)
γ, deg	90	90	97.043(5)	97.54(4)
<i>V</i> , Å ³	2249.6(2)	2302.8(4)	1169.8(1)	1157(1)
<i>Z</i>	4/2	4/2	2/2	2/2
ρ _{calcd} , g cm ⁻³	1.209	1.222	1.202	1.458
μ, mm ⁻¹	2.647	2.588	2.547	4.097
<i>F</i> (000)	872	904	452	514
	Data Collection			
2θ _{max} , deg	48	60	52	60
index ranges				
<i>h</i>	-14 to 13	0-15	-12 to 2	-12 to 14
<i>k</i>	-14 to 15	-21 to 21	-12 to 12	-14 to 14
<i>l</i>	-15 to 15	-19 to 18	-13 to 13	-16 to 15
	Solution and Refinement			
no. of rflns measd	12 013	12 766	4916	10 914
no. of indep rflns	3509 (<i>R</i> _{int} = 0.1414)	6061 (<i>R</i> _{int} = 0.1102)	4314 (<i>R</i> _{int} = 0.0404)	6684 (<i>R</i> _{int} = 0.0498)
no. of params	213	245	261	258
GOF	0.985	0.940	1.023	1.068
final <i>R</i> indices <i>R</i> ₁ , <i>wR</i> ₂				
obsd data	0.0850/0.2239	0.0558/0.1217	0.0491/0.1104	0.0358/0.0772
all data	0.1795/0.2826	0.1474/0.1493	0.1212/0.1297	0.0455/0.0809
<i>e</i> (max)/ <i>e</i> (min), e Å ⁻³	1.222/-0.716	0.688/-0.622	0.499/-0.557	1.807/-1.369

suggested on the basis of two differing Lu-C_α-C_β angles (148 and 79°).²¹

The *n*-alkyl chains adopt a zigzag chain conformation, although considerable disordering of the carbon atoms in the *n*-alkyl chain is observed. The C_α-C_β bond distances of about 1.51 Å are somewhat shortened, in agreement with such a distortion in β-agostic ethyl groups in [TiEtCl₃(dmpe)] (1.467(15) Å at 293 K;^{22b} 1.501(2) Å at 105 K^{22j}) and [Cp*Co{P(O-*p*-tolyl)₃}Et]⁺ (1.480(5) Å; Cp* = η⁵-C₅Me₅).^{22g,h} The IR spectrum of **2a** (Nujol mull, KBr) exhibits a medium intense absorption at 2730 cm⁻¹, also indicative of an agostic interaction.²³ Structural confirmation of α- and

β-agostic interactions at trivalent rare-earth metal centers still remains fairly rare. Some examples of β-agostic bonding include the permethylscandocene ethyl complex

(22) (a) Dawoodi, Z.; Green, M. L. H.; Mtetwa, V. S. B.; Prout, K. *J. Chem. Soc., Chem. Commun.* **1982**, 802. (b) Dawoodi, Z.; Green, M. L. H.; Mtetwa, V. S. B.; Prout, K.; Schultz, A. J.; Williams, J. M.; Koetzle, T. F. *J. Chem. Soc., Dalton Trans.* **1986**, 1629. (c) Jordan, R. F.; Bradley, P. K.; Baenziger, N. C.; LaPointe, R. E. *J. Am. Chem. Soc.* **1990**, *112*, 1289. (d) Fellmann, J. D.; Schrock, R. R.; Traficante, D. D. *Organometallics* **1982**, *1*, 481. (e) Fryzuk, M. D.; Johnson, S. A.; Rettig, S. J. *J. Am. Chem. Soc.* **2001**, *123*, 1602. (f) Mole, L.; Spencer, J. L.; Carr, N.; Orpen, A. G. *Organometallics* **1991**, *10*, 49. (g) Conroy-Lewis, F. M.; Mole, L.; Redhouse, A. D.; Lister, S. A.; Spencer, J. L. *J. Chem. Soc., Chem. Commun.* **1991**, 1601. (h) Cracknell, R. B.; Orpen, A. G.; Spencer, J. L. *J. Chem. Soc., Chem. Commun.* **1984**, 326. (i) Lukens, W. W. J.; Smith, M. R. I.; Andersen, R. A. *J. Am. Chem. Soc.* **1996**, *118*, 1719. (j) Scherer, W.; Priermeier, T.; Haaland, A.; Volden, H. V.; McGrady, G. S.; Downs, A. J.; Boese, R.; Bläser, D. *Organometallics* **1998**, *17*, 4406.

(21) Stern, D.; Sabat, M.; Marks, T. J. *J. Am. Chem. Soc.* **1990**, *112*, 9558.

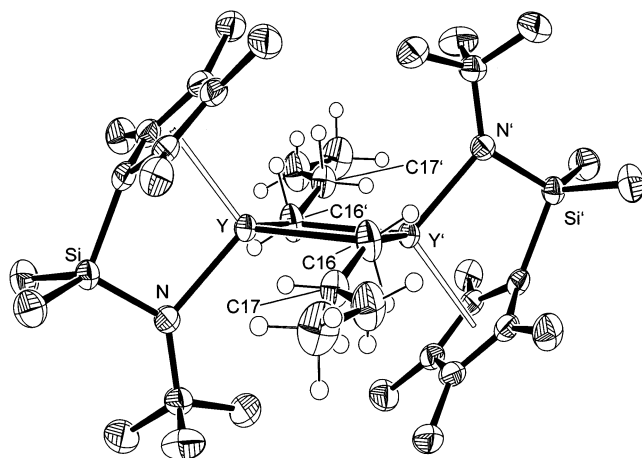


Figure 1. ORTEP diagram of the molecular structure of **2a**. Thermal ellipsoids are drawn at the 30% probability level. Hydrogen atoms, except for those on the *n*-butyl groups, are omitted for clarity. Selected bond lengths (Å) and bond angles (deg): Y–C16 = 2.542(2), Y–C16' = 2.544(2), Y–N = 2.229(1), Cp_{Cent}–Y = 2.346(5), Y...Y' = 3.5370(4), C16–C17 = 1.49(1); Y–C16–Y' = 88.14(6), C16–Y–C16' = 91.86(6), N–Y–C16 = 109.41(6), N–Y–C16' = 122.25(7), Y–C16–C17 = 84.7(5), Y'–C16–C17 = 165.3(4).

Cp*₂ScEt,^{2b} the μ -ethyl dilutetium complex [$\{\text{Et}_2\text{Si}(\eta^5\text{-C}_5\text{H}_4)(\eta^5\text{-C}_5\text{Me}_4)\text{Lu}\}_2(\mu\text{-H})(\mu\text{-Et})$],²¹ and the neopentoxide complexes [$\text{Ln}_4(\text{OCH}_2\text{CMe}_3)_4(\mu\text{-OCH}_2\text{CMe}_3)_8$] (Ln = La, Nd).²⁴

NMR Spectroscopic Data. At room temperature, the yttrium *n*-butyl complex **2a** shows overall C_{2h} symmetry, as previously reported for the *n*-hexyl complex **4a**. Only two singlets are observed in both the ¹H and ¹³C NMR spectra in toluene-*d*₈ for the eight cyclopentadienyl methyl groups and one singlet for the methyl groups on the SiMe₂ bridges. The protons of the α -carbon are observed as a broad triplet at -0.32 ppm, with the corresponding ¹³C resonance appearing as a triplet of doublets at 39.1 ppm ($^1J_{\text{YC}} = 22.3$ Hz, $^1J_{\text{CH}} = 103.3$ Hz). The centrosymmetric structure observed in the crystalline state thus undergoes some exchange process. When the temperature is lowered, the α -proton resonance undergoes decoalescence at about -5 °C, and two triplets are recorded at -20 °C (Figures 2 and 3). The triplet at higher field shows coupling of $^3J_{\text{HH}} = 3.9$ Hz to one of the β -protons at 1.14 ppm, as was verified by various techniques such as selective-decoupling experiments. It is noteworthy that only the lower field $\alpha\text{-CH}_2$ protons exhibit coupling to the yttrium atoms ($^2J_{\text{YH}} = 2$ Hz).

At first the protons of the $\beta\text{-CH}_2$ group could not be located, due to the broadness and overlap with other resonances. 2D *J*-resolved techniques, however, unambiguously allowed their assignment as two well-separated higher order multiplets at 0.87 and 1.14 ppm at room temperature. Considerable efforts have been expended to find definitive evidence for an interaction of

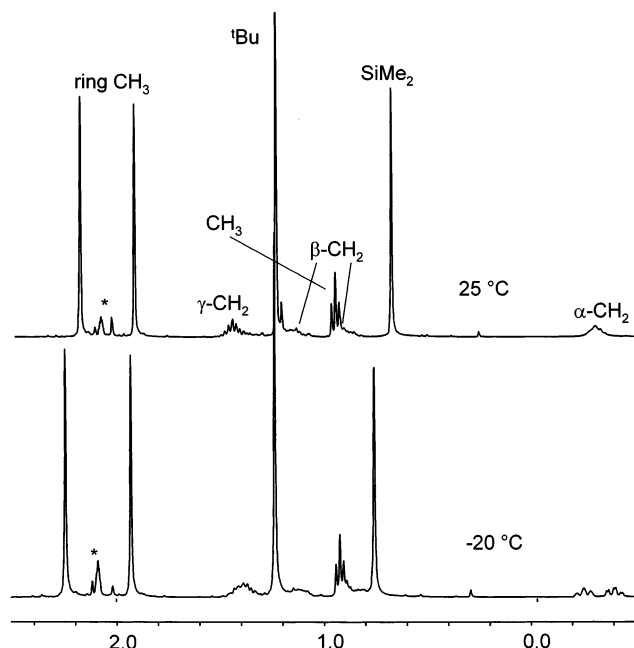


Figure 2. 400 MHz ¹H NMR spectrum of **2a** in toluene-*d*₈ at 25 and -20 °C (asterisks denote C₆D₅CD₂H).

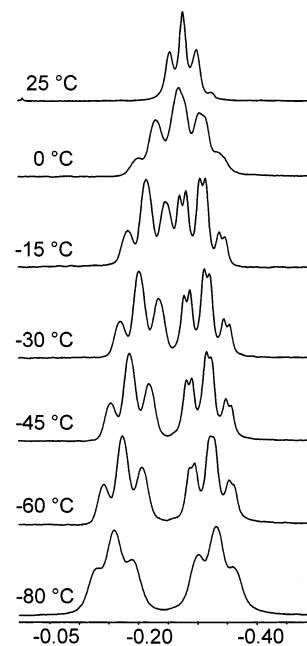
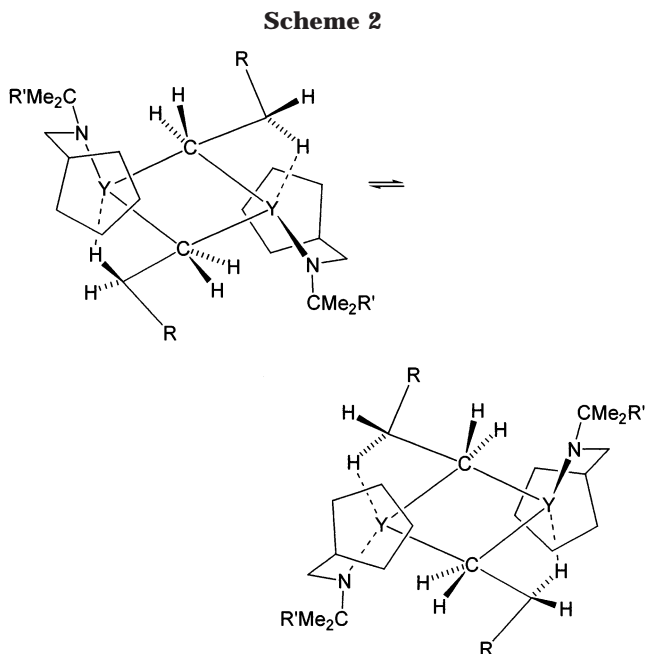


Figure 3. Temperature-dependent 400 MHz ¹H NMR spectra of **2a** in toluene-*d*₈. The region for α -proton resonances is shown.

the β -protons with the yttrium center. However, no clear-cut static effect could be found: in the ¹H NMR spectra no coupling of the β -protons to the yttrium was observed, even at -80 °C. The corresponding ¹³C resonance is recorded at 30.4 ppm with $^1J_{\text{CH}} = 114.7$ Hz. This coupling constant is smaller than that in Cp*₂ScEt, which contains a β -agostic ethyl group, where the resonance is found at 20.5 ppm with $^1J_{\text{CH}} = 120$ Hz.^{2c} For Cp*₂YCH₂CH₂CHMe₂ the significantly decreased value of $^1J_{\text{CH}} = 108$ Hz was reported as evidence for a β -agostic interaction.^{25a} In related complexes such as *trans*-[Cp*Y(OC₆H₃-^tBu₂-2,6)]₂($\mu\text{-C}_2\text{H}_3\text{R})(\mu\text{-H})$], direct coupling with $^1J_{\text{YH}}$ of about 2 Hz was found for the β -protons.²⁶

(23) For reviews on agostic interactions, see: (a) Brookhart, M.; Green, M. L. H. *J. Organomet. Chem.* **1983**, *250*, 395. (b) Brookhart, M.; Green, M. L. H.; Wong, L. L. *Prog. Inorg. Chem.* **1988**, *36*, 1. (c) Crabtree, R. H.; Hamilton, D. G. *Adv. Organomet. Chem.* **1988**, *28*, 299. (d) McGrady, G. S.; Downs, A. J. *Coord. Chem. Rev.* **2000**, *197*, 95.

(24) Barnhart, D. M.; Clark, D. L.; Gordon, J. C.; Huffman, J. C.; Watkin, J. G.; Zwick, B. D. *J. Am. Chem. Soc.* **1993**, *115*, 8461.



To perform isotope perturbation experiments,²⁷ the deuteride $[Y(\eta^5\text{-}\eta^1\text{-C}_5\text{Me}_4\text{SiMe}_2\text{NCMe}_3)(\text{THF})(\mu\text{-D})]_2$ was reacted with 1-butene to give an *n*-butyl complex with one deuterium at the β -carbon atom, $[Y(\eta^5\text{-}\eta^1\text{-C}_5\text{Me}_4\text{SiMe}_2\text{NCMe}_3)(\mu\text{-CH}_2\text{CHDEt})]_2$ (**2a-d**). It was characterized by two signals at 0.84 and 1.12 ppm in the ^2H NMR spectrum and by the signal at 30.3 ppm with $^1J_{\text{CD}} = 17.9$ Hz in the ^{13}C NMR spectrum. Temperature-dependent ^1H NMR spectroscopy, however, did not allow the detection of a significant difference in the chemical shifts in comparison with **2a** due to considerable broadening of the signals, precluding exact determination of the chemical shifts. In the temperature range from -80 up to 90 $^\circ\text{C}$, no coalescence of the $\beta\text{-CH}_2$ groups was detected. The broadening is probably due to the formation of diastereomers resulting from the "chiral" β -carbon atoms.

At this time, we can conclude that, in solution, the dimeric *n*-alkyl complexes **2–4** undergo a fluxional process, which results in the exchange of the diastereotopic α -protons and in overall C_{2h} symmetry (Scheme 2). This exchange process concomitantly results in the shifting of the $\beta\text{-CH}_2$ group from one yttrium atom to the other. In contrast to the α -protons and γ -protons, the β -protons always remain diastereotopic because of the agostic interaction. A similar process was reported for the phenoxo complexes *trans*- $[\{\text{Cp}^*\text{Y}(\text{OC}_6\text{H}_3\text{-}t\text{Bu}_2\text{-}2,6)\}_2(\mu\text{-C}_2\text{H}_3\text{R})(\mu\text{-H})]$.²⁶

Mechanism of the α -Olefin Insertion. The reactions of the dimeric hydride **1a** with α -olefins such as 1-hexene do not follow simple kinetics, since the presence of THF always results in the formation of a mixture of the dimeric alkyl complex **4a** and the monomeric THF adduct **8a** (vide infra). In neat THF and at room temperature the reaction takes place at rates inconve-

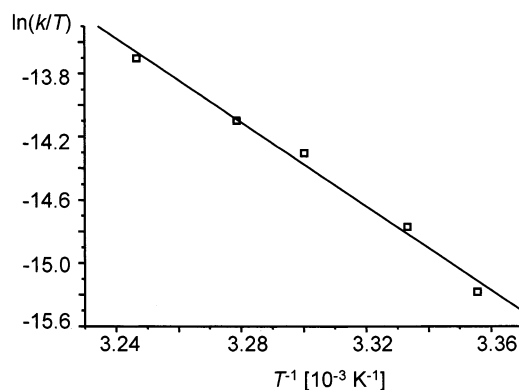


Figure 4. Eyring plot for the reaction of the hydride complex **1a** with 1-hexene in C_6D_6 .

Table 4. Rate Constants for the Reaction of **1a with 1-Hexene**

<i>T</i> (K)	<i>k</i> (10^{-5} s^{-1})	<i>T</i> (K)	<i>k</i> (10^{-5} s^{-1})
298	6.22 ± 0.05	305	18.80 ± 0.03
300	9.46 ± 0.06	308	28.18 ± 0.05
303	15.24 ± 0.01		

niently slow for NMR spectroscopic monitoring. When the reaction of the dimeric hydrides with 1-hexene was followed in toluene- d_8 in the presence of 10 equiv of THF (to ensure complete formation of **8a**), pseudo-first-order kinetics was observed. The rate constants are compiled in Table 4, and the Eyring plot is shown in Figure 4. The activation parameters were determined to be $\Delta H^\ddagger = 26 \pm 2$ kcal mol $^{-1}$ and $\Delta S^\ddagger = 11 \pm 1$ cal K $^{-1}$ mol $^{-1}$. These values can be compared to those reported for the reaction of $[\{\text{Et}_2\text{Si}(\eta^5\text{-C}_5\text{H}_4)(\eta^5\text{-C}_5\text{Me}_4)\text{Lu}\}_2(\mu\text{-H})_2]$ with 1-hexene ($\Delta H^\ddagger = 12.0 \pm 0.4$ kcal mol $^{-1}$ and $\Delta S^\ddagger = -38.6 \pm 0.7$ cal K $^{-1}$ mol $^{-1}$)²¹ or for the reaction of $[\text{Cp}^*_2\text{YH}]_2$ with 3-methyl-1-butene ($\Delta H^\ddagger = 15.8 \pm 0.2$ kcal mol $^{-1}$ and $\Delta S^\ddagger = 6 \pm 1$ cal K $^{-1}$ mol $^{-1}$).^{25a} The larger activation enthalpy may reflect the fact that the dissociation of the dinuclear hydride **1a** is a crucial step.

The dependence of the rate constants on the THF concentration remained obscure. This is due to the fact that the dissociation rates for the two THF ligands in the hydrides cannot be deduced reliably because this process is intermingled with the monomer–dimer dissociation (scrambling of the dimeric hydride occurs on the chemical time scale at room temperature).^{13b,c} Recently, considerable work on the kinetics of 1-alkene insertion reactions into the metal–hydride bonds in lanthanocene complexes such as $[\text{Cp}^*_2\text{YH}]_2$ ²⁵ revealed distinct pathways depending on the substituent of the alkene. Insertion of 1-alkene into the yttrium–hydride bond in both the dimer and monomer was inferred, and the possibility of a (slower) 1-alkene insertion in the dimer was suggested by kinetic studies.^{25b} So far we have not found conclusive evidence for the formation of a mixed alkyl–hydride complex of the type $[Y_2(\eta^5\text{-}\eta^1\text{-C}_5\text{Me}_4\text{SiMe}_2\text{NCMe}_2\text{R}')_2(\mu\text{-CH}_2\text{CH}_2\text{R})(\mu\text{-H})]$. Such complexes have been reported earlier as the sole product of 1-alkene insertion into the yttrium–hydride bond in $[\text{Cp}^*\text{Y}(\text{OC}_6\text{H}_3\text{-}t\text{Bu}_2\text{-}2,6)(\mu\text{-H})]_2$ ²⁶ or into the lutetium–hydride bond in $[\{\text{Et}_2\text{Si}(\eta^5\text{-C}_5\text{H}_4)(\eta^5\text{-C}_5\text{Me}_4)\text{Lu}\}_2(\mu\text{-H})_2]$.²¹

Finally, thermolysis of the dinuclear *n*-alkyl complexes in solution at 60 $^\circ\text{C}$ shows the formation of 1-alkene and *n*-alkane. No evidence of the formation of the hydride complex was found, indicating an undefined

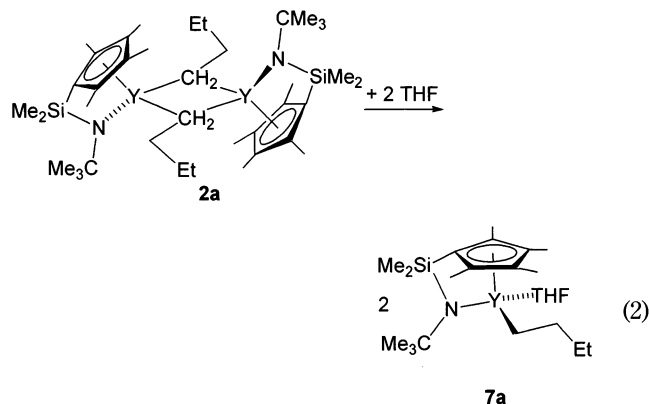
(25) (a) Casey, C. P.; Tunge, J. A.; Lee, T.-Y.; Carpenetti, D. W., II. *Organometallics* **2002**, *21*, 389. (b) Voskoboinikov, A. Z.; Shestakova, A. K.; Beletskaya, I. P. *Organometallics* **2001**, *20*, 2794.

(26) Schaverien, C. J. *Organometallics* **1994**, *13*, 69.

(27) (a) Calvert, R. B.; Shapley, J. R. *J. Am. Chem. Soc.* **1978**, *100*, 7726. (b) Green, M. L. H.; Hughes, A. K.; Popham, N. A.; Stephens, A. H.; Wong, L. L. *J. Chem. Soc., Dalton Trans.* **1992**, 3077.

decomposition rather than a clean process such as β -hydride elimination.²⁸

Reactions of the Alkyl Complexes with THF and DME. When at least 2 equiv of THF was added to a toluene solution of the *n*-butyl complex **2a**, the dimer was instantaneously converted into the mononuclear complex $[Y(\eta^5\text{-}\eta^1\text{-C}_5\text{Me}_4\text{SiMe}_2\text{NCMe}_3)(\text{CH}_2\text{CH}_2\text{Et})(\text{THF})]$ (**7a**) according to eq 2. Attempts to isolate the THF



complex **7a** remained without success, since only the starting *n*-butyl complex **2a** could be recovered from concentrated solutions. This behavior is indicative of the reversibility of the THF addition. The equilibrium constant at room temperature was estimated to be $K_{\text{eq}} = 5.0 \pm 0.5 \text{ L mol}^{-1}$ by ^1H NMR spectroscopy (19.65 mM solutions of **2a** in C_6D_6). ^1H NMR spectroscopic monitoring of the reaction of **2a** with THF shows that mononuclear units $[Y(\eta^5\text{-}\eta^1\text{-C}_5\text{Me}_4\text{SiMe}_2\text{NCMe}_3)(\text{CH}_2\text{CH}_2\text{Et})(\text{THF})]$ (**7a**) form cleanly (Figure 5). ^1H NMR spectroscopy also shows that there are no other detectable species, thus precluding the existence of the previously postulated dinuclear THF adduct $[Y(\eta^5\text{-}\eta^1\text{-C}_5\text{Me}_4\text{SiMe}_2\text{NCMe}_3)(\mu\text{-CH}_2\text{CH}_2\text{Et})(\text{THF})]_2$.^{13b}

At room temperature the spectrum is consistent with a C_s -symmetric molecule; below -80°C the chiral structure becomes apparent in both the ^1H and ^{13}C NMR spectra, since four distinct singlets for the cyclopentadienyl methyl groups as well as two singlets for the SiMe_2 group are recorded (Figure 6). In analogy with the behavior of the structurally characterized complex $[Y(\eta^5\text{-}\eta^1\text{-C}_5\text{Me}_4\text{SiMe}_2\text{NCMe}_2\text{Et})(\text{CH}_2\text{SiMe}_3)(\text{THF})]$,^{13b} this observation is consistent with the freezing out of the rapid THF dissociation at room temperature. The free energy of activation for this process is calculated by using the variable-temperature NMR data as $\Delta G^\ddagger = 9.8 \pm 0.1 \text{ kcal mol}^{-1}$. The protons at the α -carbon give rise to a multiplet at 25°C and to two separated triplets at -80°C . The resonance for the α -carbon appears in the ^{13}C NMR spectra as a doublet of triplets at 37.9 ppm with $^1J_{\text{YC}} = 53.1 \text{ Hz}$ and $^1J_{\text{CH}} = 104.3 \text{ Hz}$. The deuterium-labeled complex **2a-d**₂ similarly dissociates into the THF adduct **7a-d**₂, when treated with THF. In the ^{13}C NMR spectrum, the β -carbon is observed as a triplet with $^1J_{\text{CD}} = 18.6 \text{ Hz}$. The *n*-hexyl derivative **8a** was similarly observed by dissolving the dimer **4a** in THF- d_8 .

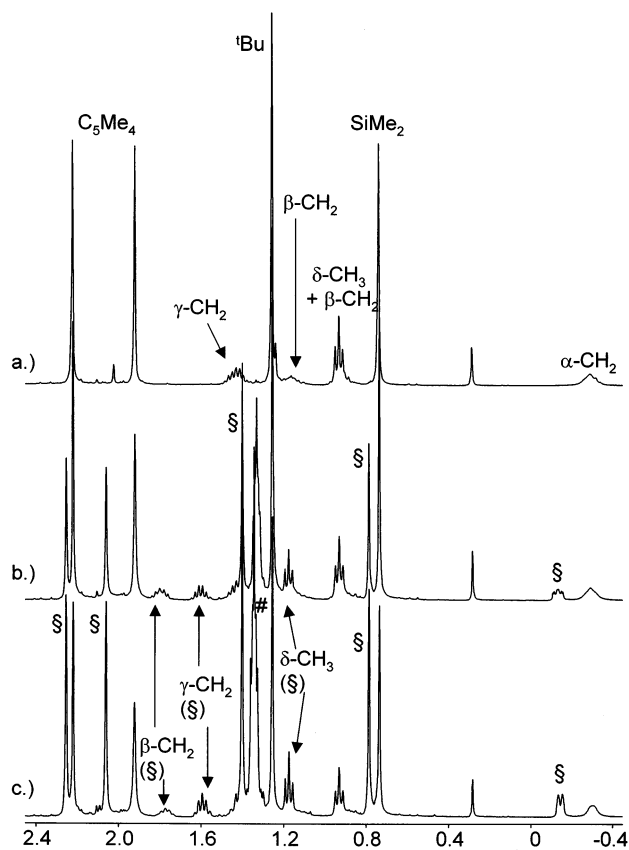


Figure 5. Reaction of **2a** with THF at 25°C in C_6D_6 : (a) pure **2a**; (b) signals after addition of 3.5 equiv of THF; (c) **2a-d**₂ after addition of 2.5 equiv of THF. Signals denoted with § are due to the THF complex **7a** and **7a-d**₂, respectively; resonances denoted with # are due to added THF (free and coordinated).

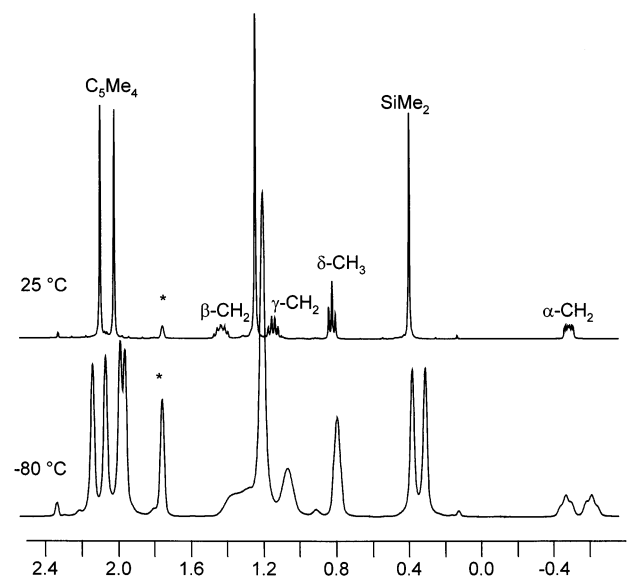
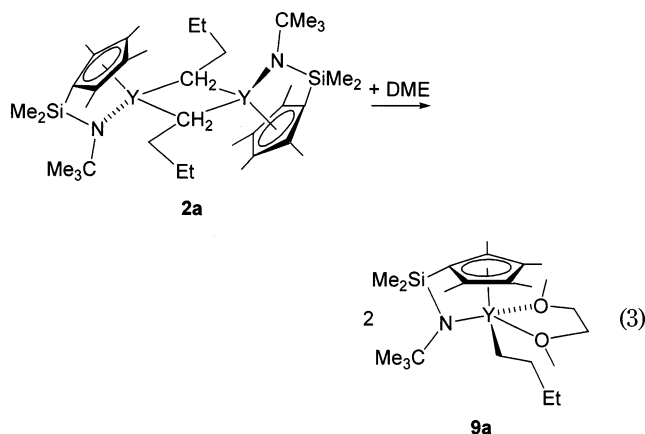


Figure 6. 400 MHz ^1H NMR spectra of **7a** in THF- d_8 at 25°C and -80°C . Resonances marked with an asterisk are due to $\text{C}_4\text{D}_7\text{HO}$.

When the dimeric *n*-butyl complex **2a** is treated with 2 equiv of 1,2-dimethoxyethane (DME), the DME adduct $[Y(\eta^5\text{-}\eta^1\text{-C}_5\text{Me}_4\text{SiMe}_2\text{NCMe}_3)(\text{CH}_2\text{CH}_2\text{Et})(\text{DME})]$ (**9a**) can be isolated as fairly thermally robust, colorless crystals

(28) For complexes resistant to β -H elimination, see e.g.: (a) Wendt, O. F.; Bercau, J. E. *Organometallics* **2001**, *20*, 3891. (b) Casey, C. P.; Fisher Klein, J.; Fagan, M. A. *J. Am. Chem. Soc.* **2000**, *122*, 4320.

(eq 3). Analogously, the *n*-hexyl complex $[Y(\eta^5\text{-}\eta^1\text{-C}_5\text{Me}_4\text{-}$



$\text{SiMe}_2\text{NCMe}_3)(\text{CH}_2\text{CH}_2^n\text{Bu})(\text{DME})$ (**10a**) can be prepared from complex **4a**.

Single crystals of **9a** suitable for X-ray diffraction were obtained by crystallization from hexane solution at -30°C . Table 1 lists the crystallographic data, and Figure 7 shows ORTEP diagrams of **9a**. The crystal structure analysis reveals square-pyramidal coordination geometry at a pseudo-five-coordinate yttrium center with a terminal *n*-butyl group in the usual zigzag conformation and a chelating DME ligand. The yttrium– α -carbon distance is 2.435(5) Å and is comparable with that in corresponding alkyl complexes with terminal *n*-alkyl groups such as $[Y(\eta^5\text{-}\eta^1\text{-C}_5\text{Me}_4\text{SiMe}_2\text{NCMe}_2\text{Et})(\text{CH}_2\text{SiMe}_3)(\text{THF})]$ (2.388(7) Å).^{13b} The angle at the α -alkyl carbon atom $Y\text{-C}_\alpha\text{-C}_\beta$ is $130.1(4)^\circ$, similar to the value of 129.7° found in $[\text{Ti}(\eta^5\text{-}\eta^1\text{-C}_5\text{Me}_4\text{SiMe}_2\text{NCMe}_3)(\text{CH}_2\text{CH}_2\text{Et})\text{Cl}]$ ²⁹ but larger than the values found in $[\text{Sc}\{\text{N}(\text{SiMe}_2\text{CH}_2\text{P}^i\text{Pr}_2)_2\}\text{Et}_2]$ ($115.5(2)^\circ$),³⁰ $[\text{Hf}(\eta^5\text{-}\eta^1\text{-}\eta^1\text{-C}_5\text{Me}_4\text{SiMe}_2\text{NCH}_2\text{CH}_2\text{OMe})(\text{CH}_2\text{CH}_2\text{Et})_2]$ ($113.4(3)$ and $117.1(3)^\circ$),^{31a} $[\text{Zr}\{\eta^5\text{-}\eta^1\text{-}\eta^1\text{-}2,6\text{-}(\text{C}_5\text{H}_4\text{CH}_2)_2\text{-C}_5\text{H}_3\text{N}\}(\text{CH}_2\text{CH}_2\text{Et})_2]$ ($122.7(6)$ and $121.4(6)^\circ$),^{31b} and $[\text{Hf}\{\text{O}(\text{CH}_2\text{CH}_2\text{N}(2,6\text{-}i\text{Pr}_2\text{C}_6\text{H}_3)_2)\text{Et}_2]$ ($112.7(2)$ and $117.1(3)^\circ$).^{31c}

The yttrium–oxygen bond lengths are within the expected range of ether coordination at trivalent yttrium.³² The yttrium–oxygen bond trans to the amidonitrogen bond is longer by 0.046 Å than the lateral bond of the DME ligand. This finding can be ascribed to the trans influence of the doubly bonded amido ligand and was previously observed in related pseudo-five-coordinate complexes such as $[Y(\eta^5\text{-}\eta^1\text{-C}_5\text{Me}_4\text{SiMe}_2\text{NCMe}_3)(2\text{-C}_4\text{H}_3\text{O})(\text{DME})]$ ($Y\text{-O} = 2.387(2)$ and $2.473(2)$ Å) and $[Y(\eta^5\text{-}\eta^1\text{-C}_5\text{Me}_4\text{SiMe}_2\text{NCMe}_3)(\eta^1\text{-}\kappa\text{-C}_4\text{H}_4\text{N})(\text{DME})]$ ($Y\text{-O} = 2.386(2)$ and $2.439(2)$ Å).³³

The weaker bonding of the “internal” yttrium–oxygen atom trans to the amidonitrogen function may be

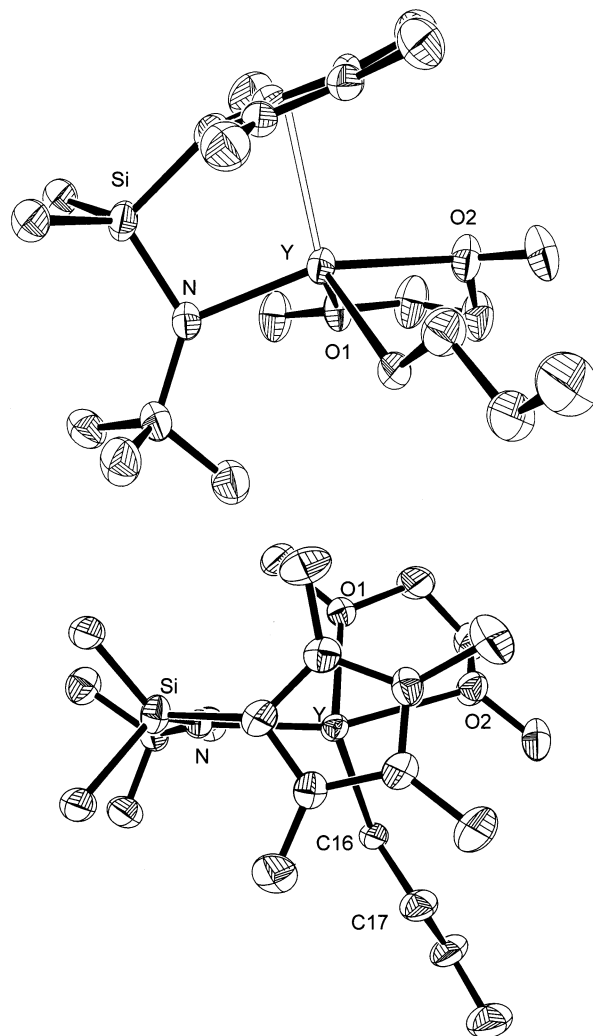


Figure 7. (a, top) ORTEP diagram of the molecular structure of **9a**. Thermal ellipsoids are drawn at the 50% probability level. Hydrogen atoms are omitted for the sake of clarity. (b, bottom) View of **9a** from the top. Selected bond lengths (Å) and bond angles (deg): $Y\text{-C16} = 2.435(5)$, $Y\text{-O1} = 2.431(3)$, $Y\text{-O2} = 2.477(3)$, $Y\text{-N} = 2.244(3)$, $\text{Cp}_{\text{Cent}}\text{-Y} = 2.366$, $\text{C16}\text{-C17} = 1.511(7)$; $\text{C16}\text{-Y}\text{-C17} = 130.1(4)$, $\text{N}\text{-Y}\text{-C16} = 103.0(2)$, $\text{N}\text{-Y}\text{-O1} = 88.8(1)$, $\text{C16}\text{-Y}\text{-O2} = 83.7(2)$.

responsible for the fluxional behavior of the DME adduct, as studied by variable-temperature ^1H NMR spectroscopy (Figure 8). No exchange with free DME can be observed at room temperature, even in the presence of a large excess of DME, as suggested by the preservation of C_1 symmetry. A strong temperature dependence of the methoxy and methylene signals is detected. The resonance assigned to both OMe groups at 3.04 ppm at 25°C decoalesces upon lowering the temperature to $T_c = -35^\circ\text{C}$. At -70°C two singlets at 2.80 and 3.07 ppm are observed. The free energy of activation for this process is $\Delta G^\ddagger = 11.2 \pm 0.1$ kcal mol $^{-1}$. Most strikingly, the chirality of the yttrium center is retained throughout the whole temperature range up to 25°C . Thus, the two methyl resonances of the SiMe_2 group remain inequivalent, and four separate singlets are observed for the C_5Me_4 ligand. This feature can only be explained if the fluxionality of the coordinated DME ligand involves either a nondissociative pseudorotation process or dissociation of one yttrium–oxygen bond via

(29) Millward, D. B.; Cole, A. P.; Waymouth, R. M. *Organometallics* **2000**, *19*, 1870.

(30) Fryzuk, M. D.; Rettig, S. J. *Organometallics* **1996**, *15*, 3329.

(31) (a) Amor, F.; Spaniol, T. P.; Okuda, J. *Organometallics* **1997**, *16*, 4765. (b) Paolucci, G.; Projana, G.; Zanon, J.; Lucchini, V.; Avtomonov, E. *Organometallics* **1997**, *16*, 5312. (c) Aizenberger, M.; Turculet, L.; Davis, W. M.; Schattenmann, F.; Schrock, R. R. *Organometallics* **1998**, *17*, 4795.

(32) (a) $\text{Cp}^*\text{YMe}(\text{THF})$: $Y\text{-O} = 2.379(8)$ Å. See: den Haan, K. H.; de Boer, J. L.; Teuben, J. H.; Smeets, W. J. J.; Spek, A. L. *J. Organomet. Chem.* **1987**, *327*, 31. (b) $\text{Cp}^*\text{Y}(\text{CH}_2\text{Ph})(\text{THF})$: $Y\text{-O} = 2.398(4)$ Å. See: Mandel, A.; Magull, J. *Z. Anorg. Allg. Chem.* **1996**, *622*, 1913.

(33) Arndt, S.; Trifonov, A. A.; Spaniol, T. P.; Okuda, J.; Kitamura, M.; Takahashi, T. *J. Organomet. Chem.* **2002**, *647*, 158.

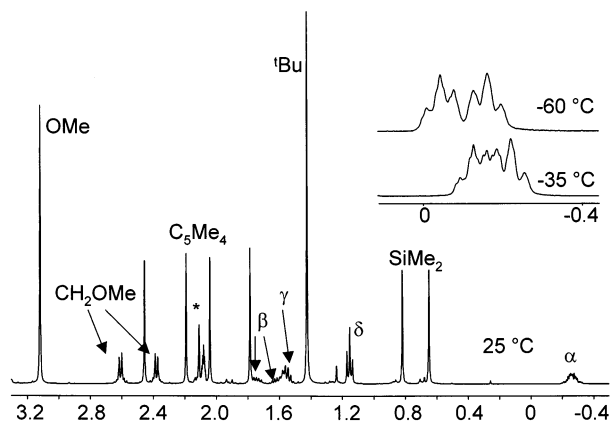
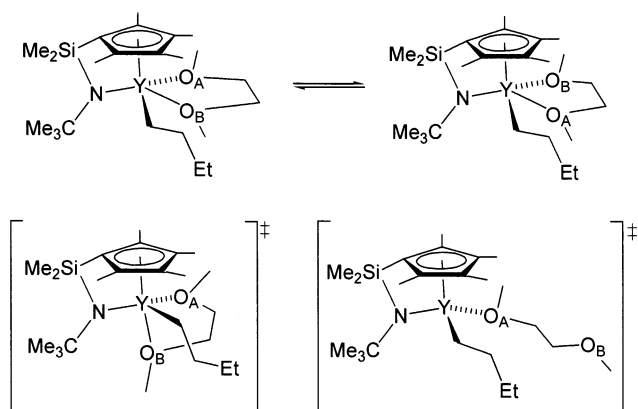


Figure 8. 400 MHz ^1H NMR spectrum of **9a** in toluene- d_8 at 25 $^\circ\text{C}$ (the asterisk denotes $\text{C}_6\text{D}_5\text{CD}_2\text{H}$). The insert shows the α -proton region at -35 and -60 $^\circ\text{C}$.

Scheme 3



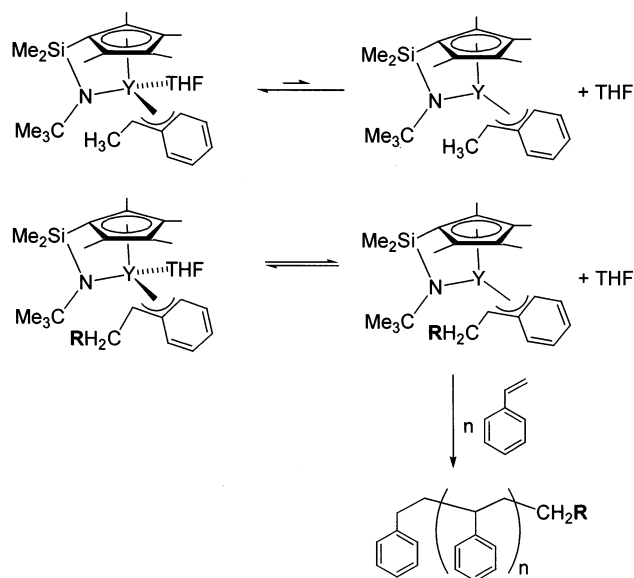
a configurationally *stable* tetrahedral intermediate (Scheme 3).³⁴

Conclusion

We suggest that the controlled polymerization of styrene by the yttrium hydride complex $[\text{Y}(\eta^5\text{:}\eta^1\text{-C}_5\text{Me}_4\text{-SiMe}_2\text{NCMe}_2\text{R}')(\text{THF})(\mu\text{-H})_2]$ which has been activated by the 1-alkene $\text{H}_2\text{C}=\text{CHR}$ ^{13b} involves the formation of a THF adduct of the monoinsertion product, $[\text{Y}(\eta^5\text{:}\eta^1\text{-C}_5\text{Me}_4\text{-SiMe}_2\text{NCMe}_2\text{R}')(\text{CH}_2\text{CH}_2\text{R})(\text{THF})]$, in a first step. Under standard conditions (100-fold excess of styrene, 25 $^\circ\text{C}$, toluene), only this THF adduct of the *n*-alkyl complex $[\text{Y}(\eta^5\text{:}\eta^1\text{-C}_5\text{Me}_4\text{-SiMe}_2\text{NCMe}_2\text{R}')(\text{CH}_2\text{CH}_2\text{R})(\text{THF})]$ is capable of polymerizing styrene. Neither the dimeric alkyl complexes $[\text{Y}(\eta^5\text{:}\eta^1\text{-C}_5\text{Me}_4\text{-SiMe}_2\text{NCMe}_2\text{R}')(\mu\text{-CH}_2\text{CH}_2\text{R})_2]$ nor the DME adduct $[\text{Y}(\eta^5\text{:}\eta^1\text{-C}_5\text{Me}_4\text{-SiMe}_2\text{NCMe}_2\text{R}')(\text{CH}_2\text{CH}_2\text{R})(\text{DME})]$ nor the (trimethylsilyl)methyl complex $[\text{Y}(\eta^5\text{:}\eta^1\text{-C}_5\text{Me}_4\text{-SiMe}_2\text{NCMe}_2\text{R}')(\text{CH}_2\text{-SiMe}_3)(\text{THF})]$ ^{13a,b} initiates styrene polymerization. The failure of the dimeric *n*-alkyl complex $[\text{Y}(\eta^5\text{:}\eta^1\text{-C}_5\text{Me}_4\text{-SiMe}_2\text{NCMe}_2\text{R}')(\mu\text{-CH}_2\text{CH}_2\text{R})_2]$ to undergo further insertion of α -olefins is due to the relatively high stability of the dimeric structure, where the β -agostic interaction of the bridging alkyl groups alleviates the metal's electrophilicity. The lability of the THF in $[\text{Y}(\eta^5\text{:}\eta^1\text{-C}_5\text{Me}_4\text{-SiMe}_2\text{NCMe}_2\text{R}')(\text{CH}_2\text{CH}_2\text{R})(\text{THF})]$ allows the styrene monomer to approach the yttrium center and insert into the *n*-alkyl bond.³⁵

(34) For the stereochemistry of five-coordinate complexes, see: Brunner, H. *Adv. Organomet. Chem.* **1980**, *18*, 151.

Scheme 4



The reason the isolable 1-phenethyl product $[\text{Y}(\eta^5\text{:}\eta^1\text{-C}_5\text{Me}_4\text{-SiMe}_2\text{NCMe}_2\text{R}')\{\text{CH}(\text{Ph})\text{CH}_3\}(\text{THF})]$, formed by styrene monoinsertion into the yttrium–hydride bond of the hydride complex,^{13b} does not undergo further styrene insertion can be ascribed to two factors. One is the decreased electrophilicity at the yttrium center due to the (fluxional) η^3 coordination of the 1-phenethyl group. More importantly, however, the lability of the THF ligand toward styrene coordination in $[\text{Y}(\eta^5\text{:}\eta^1\text{-C}_5\text{Me}_4\text{-SiMe}_2\text{NCMe}_2\text{R}')\{\text{CH}(\text{Ph})\text{CH}_2\text{R}\}(\text{THF})]$ ($\text{R} = \text{H}$, *n*-alkyl, polystyryl) appears to critically depend on the nature of **R**. Obviously the (seemingly small) increase in the alkyl group's steric requirement derived from styrene insertion into the *n*-alkyl ligand in $[\text{Y}(\eta^5\text{:}\eta^1\text{-C}_5\text{Me}_4\text{-SiMe}_2\text{NCMe}_2\text{R}')\{\text{CH}(\text{Ph})\text{CH}_2\text{R}\}(\text{THF})]$ is sufficient to labilize THF to the extent that polymerization of styrene can occur (Scheme 4). We will report in a separate contribution on the details of the livingness, 2,1-regioselectivity, and syndiospecificity of this type of styrene polymerization.³⁶

Experimental Section

General Considerations. All operations were performed under an inert atmosphere of argon using standard Schlenk-line or glovebox techniques. After drying over KOH, THF was distilled from sodium benzophenone ketyl. Hexane and toluene were purified by distillation from sodium/triglyme benzophenone ketyl. Anhydrous trichlorides of ytterbium and yttrium (ALFA or Strem) were used as received. The hydride complexes $[\text{Y}(\eta^5\text{:}\eta^1\text{-C}_5\text{Me}_4\text{-SiMe}_2\text{NCMe}_2\text{R}')(\text{THF})(\mu\text{-H})_2]$ (**1a**, $\text{R} = \text{Me}$; **1b**, $\text{R} = \text{Et}$) and $[\text{Yb}(\eta^5\text{:}\eta^1\text{-C}_5\text{Me}_4\text{-SiMe}_2\text{NCMe}_3)(\text{THF})(\mu\text{-H})_2]$ (**5a**) were prepared according to published procedures.^{13a,b} All other

(35) (a) A somewhat similar acceleration effect by THF can be found for the yttrium-catalyzed hydrosilylation of 1-alkenes: den Haan, K. H.; Wielstra, Y.; Teuben, J. H. *Organometallics* **1987**, *6*, 2053. Molander, G. A.; Dowdy, E. D. In *Lanthanides: Chemistry and Use in Organic Synthesis*; Kobayashi, S., Ed.; Springer: Berlin, 1999; p 119. Originally this effect was reported for the hydroboration: Wang, K. K.; Brown, H. C. *J. Am. Chem. Soc.* **1982**, *104*, 7148. (b) In the kinetic sense, the THF-free dimeric alkyl complex should also react with styrene in hydrocarbon solvents, if the rate of dissociation into monomeric units is sufficiently fast. NMR spectroscopic scrambling experiments with two different alkyl complexes rule out this possibility, at least at lower temperatures.

(36) Beckerle, K.; Okuda, J. Manuscript in preparation.

chemicals were commercially available and used after appropriate purification. NMR spectra were recorded on a Bruker DRX 400 spectrometer (^1H , 400 MHz; ^{13}C , 101 MHz; ^{29}Si , 79.5 MHz) in C_6D_6 at 25 °C, unless otherwise stated. Chemical shifts for ^1H and ^{13}C spectra were referenced internally using the residual solvent resonances and reported relative to tetramethylsilane. ^{29}Si spectra were referenced externally to tetramethylsilane. Elemental analyses were performed by the Microanalytical Laboratory of this department. In many cases the results were not satisfactory, and the best values from repeated runs were given. Moreover, the results were inconsistent from run to run and therefore not reproducible. We ascribe this difficulty, observed also by other workers,³⁷ to the extreme sensitivity of the material.

[Y(η^5 : η^1 -C₅Me₄SiMe₂NCMe₃)(μ -CH₂CH₂Et)]₂ (2a). To a solution of [Y(η^5 : η^1 -C₅Me₄SiMe₂NCMe₃)(THF)(μ -H)]₂ (**1a**; 160 mg, 194 μmol) in toluene (2 mL) was added liquid 1-butene (1.32 g, 23.5 mmol) at -78 °C. After the addition of 1-butene the cooling bath was removed and the solution was stirred at room temperature for 2 h. The reaction mixture was concentrated in vacuo and cooled to -30 °C to afford colorless crystals in two crops (100 mg, 63%). ^1H NMR (toluene-*d*₆, 25 °C): δ -0.32 (br m, 2 H, α -CH₂), 0.68 (s, 6 H, SiCH₃), 0.87 (m, 1 H, β -CH₂), 0.95 (t, $^3J_{\text{HH}} = 7.2$ Hz, 3 H, δ -CH₃), 1.14 (m, 1 H, β -CH₂), 1.24 (s, 9 H, C(CH₃)₃), 1.45 (q, $^3J_{\text{HH}} = 7.2$ Hz, 2 H, γ -CH₂), 1.92, 2.18 (s, 2 \times 6 H, C₅Me₄). $^{13}\text{C}\{^1\text{H}\}$ NMR (toluene-*d*₆, 25 °C): δ 8.1 ($^1J_{\text{CH}} = 118.1$ Hz, SiCH₃), 11.4, 14.3 ($^1J_{\text{CH}} = 125.6$ Hz, ring CH₃), 13.6 ($^1J_{\text{CH}} = 122.9$ Hz, δ -CH₃), 30.1 ($^1J_{\text{CH}} = 124.2$ Hz, γ -CH₂), 30.4 ($^1J_{\text{CH}} = 114.7$ Hz, β -CH₂), 36.1 ($^1J_{\text{CH}} = 123.5$ Hz, C(CH₃)₃), 39.1 (t, $^1J_{\text{YC}} = 22.3$ Hz, $^1J_{\text{CH}} = 103.3$ Hz, α -CH₂), 54.1 (C(CH₃)₃), 108.6 (ring C attached to SiMe₂), 123.3, 126.7 (ring C). $^{29}\text{Si}\{^1\text{H}\}$ NMR (toluene-*d*₆, 25 °C): δ -24.9. ^1H NMR (toluene-*d*₆, 90 °C): δ -0.31 (tt, $^3J_{\text{HH}} = 9.0$ Hz, $^2J_{\text{YH}} = 1.6$ Hz, 2 H, α -CH₂), 0.61 (s, 6 H, SiCH₃), 0.96 (t, $^3J_{\text{HH}} = 7.5$ Hz, 3 H, δ -CH₃), 1.01, 1.22 (m, 2 \times 1 H, β -CH₂), 1.23 (s, 9 H, C(CH₃)₃), 1.48 (m, 2 H, γ -CH₂), 1.92, 2.14 (s, 2 \times 6 H, C₅Me₄). Anal. Calcd for C₃₈H₇₂N₂Si₂Y₂: C, 57.70; H, 9.18; N, 3.54. Found: C, 57.71; H, 9.14; N, 3.44.

[Y(η^5 : η^1 -C₅Me₄SiMe₂NCMe₃)(μ -CH₂CHDEt)]₂ (2a-d₂). This complex was prepared in the same manner as **2a** by using the deuteride [Y(η^5 : η^1 -C₅Me₄SiMe₂NCMe₃)(THF)(μ -D)]₂ (**1a-d₂**; 309 mg, 0.4 mmol) to give 140 mg (50%) of **2a-d₂**. ^1H NMR (toluene-*d*₆, 25 °C): δ -0.33 (br m, 2 H, α -CH₂), 0.68 (s, 6 H, SiCH₃), 0.87 (m, 1 H, β -CH₂), 0.95 (t, $^3J_{\text{HH}} = 7.0$ Hz, 3 H, δ -CH₃), 1.12 (m, 1 H, β -CH₂), 1.24 (s, 9 H, C(CH₃)₃), 1.42 (m, 2 H, γ -CH₂), 1.92, 2.18 (s, 2 \times 6 H, C₅Me₄). $^{13}\text{C}\{^1\text{H}\}$ NMR (toluene-*d*₆, 25 °C): δ 8.2 (SiCH₃), 11.6, 14.5 (ring CH₃), 13.8 (δ -CH₃), 30.2 (γ -CH₂), 30.3 (t, $^1J_{\text{CD}} = 17.9$ Hz, β -CH₂), 36.3 (C(CH₃)₃), 39.2 (t, $^1J_{\text{YC}} = 21.8$ Hz, α -CH₂), 54.3 (C(CH₃)₃), 108.6 (ring C attached to SiMe₂), 123.5, 126.9 (ring C). ^2H NMR: δ 0.84 (m), 1.12 (m).

[Y(η^5 : η^1 -C₅Me₄SiMe₂NCMe₂Et)(μ -CH₂CH₂Et)]₂ (2b). [Y(η^5 : η^1 -C₅Me₄SiMe₂NCMe₂Et)(THF)(μ -H)]₂ (**1b**; 96 mg, 113 μmol) was dissolved in toluene (1.5 mL), and liquid 1-butene was added (0.98 g, 17.5 mmol) at -78 °C. The reaction mixture was stirred for 2 h at room temperature and the solution concentrated in vacuo. When the temperature was lowered to -30 °C, colorless crystals were isolated after washing with pentane (45 mg, 49%). ^1H NMR: δ -0.30 (br m, 2 H, α -CH₂), 0.73 (s, 6 H, SiCH₃), 0.94 (t, 7 H, $^3J_{\text{HH}} = 7.2$ Hz, 6 H, δ -CH₃ + C(CH₃)₂CH₂CH₃ + β -CH₂), 1.17 (m, 1 H, β -CH₂), 1.19 (s, 6 H, C(CH₃)₂), 1.43 (m, 2 H, γ -CH₂), 1.47 (q, 2 H, C(CH₃)₂CH₂CH₃), 1.93, 2.23 (s, 2 \times 6 H, C₅Me₄). $^{13}\text{C}\{^1\text{H}\}$ NMR: δ 8.3 (SiCH₃), 10.4 (C(CH₃)₂CH₂CH₃), 11.6, 14.6 (ring CH₃), 13.7 (δ -CH₃), 30.2 (γ -CH₂), 30.6 (β -CH₂), 32.4 (C(CH₃)₂), 39.2 (t, $^1J_{\text{YC}} = 21.7$ Hz, α -CH₂), 40.6 (C(CH₃)₂CH₂CH₃), 56.9 (C(CH₃)₂CH₂CH₃), 108.8 (ring C attached to SiMe₂), 123.6, 126.8 (ring C). Anal. Calcd for C₄₀H₇₆N₂Si₂Y₂: C, 58.66; H, 9.35; N, 3.42. Found: C, 57.13; H, 9.35; N, 5.57.

[Y(η^5 : η^1 -C₅Me₄SiMe₂NCMe₃)(μ -CH₂CH₂ⁿPr)]₂ (3a). To a solution of **1a** (70 mg, 85 μmol) in toluene (1.5 mL) was added 1-pentene (1.5 mL, 13.7 mmol) at room temperature. After it was stirred for 1 h, the solution was concentrated in vacuo and cooled to -30 °C. The product was obtained from the reaction mixture as colorless crystals (42 mg, 60%). ^1H NMR: δ -0.26 (br t, 2 H, α -CH₂), 0.75 (s, 6 H, SiCH₃), 0.89 (t, 3 H, $^3J_{\text{HH}} = 7.2$ Hz, ϵ -CH₃), 0.96, 1.23 (m, 2 \times 1 H, β -CH₂), 1.27 (s, 9 H, C(CH₃)₃), 1.39, 1.45 (m, 2 \times 2 H, γ -CH₂ + δ -CH₂), 1.94, 2.24 (s, 2 \times 6 H, C₅Me₄). $^{13}\text{C}\{^1\text{H}\}$ NMR: δ 8.3 (SiCH₃), 11.6, 14.5 (ring CH₃), 14.1 (ϵ -CH₃), 22.6 (δ -CH₂), 28.0 (γ -CH₂), 36.3 (C(CH₃)₃), 39.6 (β -CH₂), 39.8 (t, $^1J_{\text{YC}} = 23.9$ Hz, α -CH₂), 54.3 (C(CH₃)₃), 108.8 (ring C attached to SiMe₂), 123.5, 126.9 (ring C). ^1H NMR (toluene-*d*₆, -80 °C): δ -0.33, -0.16 (br t, 2 \times 1 H, α -CH₂), 0.87 (m, 4 H, β -CH₂ + ϵ -CH₃), 0.90 (s, 6 H, SiCH₃), 1.28 (s, 9 H, C(CH₃)₃), 1.33 (m, 5 H, β -CH₂ + γ -CH₂ + δ -CH₂), 1.96, 2.35 (s, 2 \times 6 H, C₅Me₄). Anal. Calcd for C₄₀H₇₆N₂Si₂Y₂: C, 58.66; H, 9.35; N, 3.42. Found: C, 58.02; H, 8.82; N, 3.89.

[Y(η^5 : η^1 -C₅Me₄SiMe₂NCMe₂Et)(μ -CH₂CH₂ⁿPr)]₂ (3b). The hydride **1b** (140 mg, 164 μmol) was dissolved in toluene (2 mL), and 1-pentene was added (2 mL, 18.3 mmol). The reaction mixture was stirred for 1 h at room temperature. The solution was concentrated in vacuo and cooled to -30 °C. The product was isolated as colorless crystals after washing with pentane (80 mg, 58%). ^1H NMR: δ -0.25 (br t, 2 H, α -CH₂), 0.73 (s, 6 H, Si(CH₃)₂), 0.90, 0.95 (t, 7 H, $^3J_{\text{HH}} = 7.2$ Hz, C(CH₃)₂CH₂CH₃ + ϵ -CH₃ + β -CH₂), 1.21 (s, 6 H, C(CH₃)₂), 1.24 (m, 1 H, β -CH₂), 1.38 (m, 4 H, γ -CH₂ + δ -CH₂), 1.48 (q, 2 H, C(CH₃)₂CH₂CH₃), 1.95, 2.25 (s, 2 \times 6 H, C₅Me₄). $^{13}\text{C}\{^1\text{H}\}$ NMR: δ 8.3 (SiCH₃), 10.6 (C(CH₃)₂CH₂CH₃), 11.6, 14.5 (ring CH₃), 14.2 (ϵ -CH₃), 22.7 (δ -CH₂), 28.2 (γ -CH₂), 36.3 (C(CH₃)₂), 39.5 (t + s, $^1J_{\text{YC}} = 23.2$ Hz, α -CH₂ + β -CH₂), 40.0 (C(CH₃)₂CH₂CH₃), 56.9 (C(CH₃)₂-CH₂CH₃), 109.9 (ring C attached to SiMe₂), 123.6, 126.3 (ring C). Anal. Calcd for C₄₂H₈₀N₂Si₂Y₂: C, 59.55; H, 9.52; N, 3.31. Found: C, 59.42; H, 9.46; N, 3.22.

[Y(η^5 : η^1 -C₅Me₄SiMe₂NCMe₃)(μ -CH₂CH₂ⁿBu)]₂ (4a). To a solution of **1a** (57 mg, 69 μmol) in toluene (1.2 mL) was added 1-hexene (1.5 mL, 12.1 mmol) at room temperature. After it was stirred for 2 h, the solution was concentrated in vacuo and cooled to -30 °C. The product (20 mg) was obtained from the reaction mixture as colorless crystals in 34% yield. ^1H NMR: δ -0.24 (br t, 2 H, α -CH₂), 0.75 (s, 6 H, SiCH₃), 0.90 (t, $^3J_{\text{HH}} = 7.2$ Hz, 3 H, ζ -CH₃), 0.98 (m, 1 H, β -CH₂), 1.28 (s, 10 H, C(CH₃)₃ + β -CH₂), 1.30, 1.39, 1.49 (m, 3 \times 2 H, γ -CH₂ + δ -CH₂ + ϵ -CH₂), 1.96, 2.25 (s, 2 \times 6 H, C₅Me₄). $^{13}\text{C}\{^1\text{H}\}$ NMR: δ 8.3 ($^1J_{\text{CH}} = 117.4$ Hz, SiCH₃), 11.6, 14.5 ($^1J_{\text{CH}} = 123.5$ + 123.3 Hz ring CH₃), 14.2 ($^1J_{\text{CH}} = 123.6$ Hz, ζ -CH₃), 22.8 ($^1J_{\text{CH}} = 126.3$ Hz, ϵ -CH₂), 28.3 ($^1J_{\text{CH}} = 118.3$ Hz, δ -CH₂), 31.6 ($^1J_{\text{CH}} = 123.0$ Hz, γ -CH₂), 36.2 ($^1J_{\text{CH}} = 123.7$ Hz, C(CH₃)₃), 36.9 (β -CH₂), 39.8 (t, $^1J_{\text{YC}} = 22.0$ Hz, $^1J_{\text{CH}} = 104.3$ Hz, α -CH₂), 54.3 (C(CH₃)₃), 108.8 (ring C attached to SiMe₂), 123.5, 126.8 (ring C). $^{29}\text{Si}\{^1\text{H}\}$ NMR: δ -24.9. Anal. Calcd for C₄₂H₈₀N₂Si₂Y₂: C, 59.55; H, 9.52; N, 3.31. Found: C, 59.30; H, 9.51; N, 3.46.

[Y(η^5 : η^1 -C₅Me₄SiMe₂NCMe₂Et)(μ -CH₂CH₂ⁿBu)]₂ (4b). The hydride **1b** was dissolved in toluene (1.5 mL), and 1-hexene was added (1.5 mL, 12.1 mmol). The reaction mixture was stirred for 2 h at room temperature. The solution was concentrated in vacuo and cooled to -30 °C to give colorless crystals after washing with pentane (46 mg, 48%). ^1H NMR: δ -0.23 (br t, 2 H, α -CH₂), 0.73 (s, 6 H, SiCH₃), 0.91, 0.96 (t, $^3J_{\text{HH}} = 7.2$ Hz, $^3J_{\text{HH}} = 7.4$ Hz, 7 H, ζ -CH₃ + C(CH₃)₂CH₂CH₃ + β -CH₂), 1.22 (s, 6 H, C(CH₃)₂), 1.31 (m, 3 H, β -CH₂ + ϵ -CH₂), 1.40, 1.46 (m, 2 \times 2 H, γ -CH₂ + δ -CH₂), 1.50 (q, 2 H, $^3J_{\text{HH}} = 7.4$ Hz, C(CH₃)₂CH₂CH₃), 1.97, 2.27 (s, 2 \times 6 H, C₅Me₄). $^{13}\text{C}\{^1\text{H}\}$ NMR: δ 8.3 (SiCH₃), 10.5 (C(CH₃)₂CH₂CH₃), 11.7, 14.6 (ring CH₃), 14.2 (ζ -CH₃), 22.8 (ϵ -CH₂), 28.4 (δ -CH₂), 31.5 (γ -CH₂), 33.5 (C(CH₃)₂), 36.9 (β -CH₂), 39.5 (t, $^1J_{\text{YC}} = 21.6$ Hz, α -CH₂), 40.6 (C(CH₃)₂CH₂CH₃), 57.0 (C(CH₃)₂), 108.8 (ring C attached to SiMe₂), 123.6, 126.7 (ring C). Anal. Calcd for C₄₄H₈₄N₂Si₂Y₂: C, 60.39; H, 9.67; N, 3.20. Found: C, 60.49; H, 9.66; N, 3.35.

(37) Mitchell, J. P.; Hajela, S.; Brookhart, S. K.; Hardcastle, K. I.; Henling, L. M.; Bercaw, J. E. *J. Am. Chem. Soc.* **1996**, *118*, 1045.

[Yb(η^5 : η^1 -C₅Me₄SiMe₂NCMe₃)(μ -CH₂CH₂^{*n*}Bu)]₂ (6a). A solution of orange [Yb(η^5 : η^1 -C₅Me₄SiMe₂NCMe₃)(THF)(μ -H)]₂ (**5a**; 30 mg, 33 μ mol) in 1 mL of benzene was treated with 1-hexene (24 μ L, 190 μ mol). The reaction turned dark red after stirring for 6 h. All volatiles were removed in vacuo, the residue was dissolved in 1 mL of hexane/benzene (1:10), the solution was filtered, and the filtrate was concentrated until incipient turbidity. After standing for 10 days at room temperature, dark red crystals suitable for crystallographic analysis were obtained (23 mg, 70%).

[Y(η^5 : η^1 -C₅Me₄SiMe₂NCMe₃)(CH₂CH₂Et)(THF)] (7a). When the dimeric alkyl **2a** was dissolved in THF-*d*₈ or when excess (>10 equiv) THF was added to a solution of **2a** in toluene or benzene, the monomeric THF adduct formed. All efforts to isolate this complex by crystallizing at -20 °C or removing the solvent in vacuo resulted in the recovery of the starting material **2a**. ¹H NMR (THF-*d*₈, 25 °C): δ -0.52 (br m, 2H, α -CH₂), 0.36 (s, 6 H, SiCH₃), 0.78 (t, ³J_{HH} = 7.4 Hz, 3 H, δ -CH₃), 1.10 (sextet, ³J_{HH} = 7.4 + 6.8 Hz, 2 H, γ -CH₂), 1.21 (s, 9 H, C(CH₃)₃), 1.39 (m, 2 H, β -CH₂), 1.98, 2.06 (s, 2 \times 6 H, C₅Me₄). ¹³C{¹H} NMR (THF-*d*₈, 25 °C): δ 8.8 (¹J_{CH} = 116.3 Hz, SiCH₃), 11.6, 14.5 (¹J_{CH} = 124.7 Hz, ring CH₃), 14.1 (¹J_{CH} = 123.5 Hz, δ -CH₃), 32.7 (¹J_{CH} = 123.5 Hz, γ -CH₂), 34.8 (¹J_{CH} = 120.2 Hz, β -CH₂), 35.6 (¹J_{CH} = 123.3 Hz, C(CH₃)₃), 37.9 (d, ¹J_{YC} = 53.1 Hz, ¹J_{CH} = 104.3 Hz, α -CH₂), 54.2 (C(CH₃)₃), 108.7 (ring C attached to SiMe₂), 120.9, 125.6 (ring C). ²⁹Si{¹H} NMR (THF-*d*₈, -80 °C): δ -28.9 (d, ¹J_{YSi} = 1.4 Hz). ¹H NMR (THF-*d*₈, -80 °C): δ -0.51, -0.65 (br m, 2 \times 1 H, α -CH₂), 0.27, 0.34 (s, 2 \times 3 H, SiCH₃), 0.75 (br s, 3 H, δ -CH₃), 1.03 (br s, 2 H, γ -CH₂), 1.17 (s, 9 H, C(CH₃)₃), 1.39 (m, 2 H, β -CH₂), 1.92, 1.95, 2.03, 2.10 (s, 4 \times 3 H, C₅Me₄). ¹³C{¹H} NMR (THF-*d*₈, -80 °C): δ 9.0, 9.5 (SiCH₃), 12.1, 12.2, 14.3, 15.6 (ring CH₃), 14.9 (δ -CH₃), 34.1 (γ -CH₂), 35.3 (C(CH₃)₃), 35.7 (β -CH₂), 37.9 (br d, ¹J_{YC} = 55.3 Hz, α -CH₂), 54.2 (N(C(CH₃)₃)), 105.8 (ring C attached to SiMe₂), 118.6, 121.4, 124.7, 125.3 (ring C).

[Y(η^5 : η^1 -C₅Me₄SiMe₂NCMe₃)(CH₂CHDEt)(THF)] (7a-d₂). In an NMR tube **2a-d₂** (11 mg, 14 μ mol) was dissolved and THF (3 μ L, 33 μ mol) was added. The NMR spectra showed the signal set for **2a-d₂** and another set ascribed to the monomeric THF adduct **7a-d₂** in the approximate ratio **2a-d₂**:**7a-d₂** = 1:0.7 by integrating the α -CH₂ protons. ¹H NMR: δ -0.14 (br d, ³J_{HH} = 12 Hz, 2 H, α -CH₂), 0.79 (s, 6 H, SiCH₃), 0.95 (t, ³J_{HH} = 7.0 Hz, 3 H, δ -CH₃), 1.32 (m, 4 H, β -CH₂, THF), 1.40 (s, 9 H, C(CH₃)₃), 1.59 (m, 2 H, γ -CH₂), 1.77 (m, 1 H, β -CH₂), 2.06, 2.25 (s, 2 \times 6 H, C₅Me₄), 3.50 (m, 4H, α -CH₂, THF). ¹³C{¹H} NMR: δ 8.5 (SiCH₃), 11.2, 14.4 (ring CH₃), 13.7 (δ -CH₃), 25.6 (β -CH₂, THF), 31.7 (γ -CH₂), 32.9 (t, ¹J_{CD} = 18.6 Hz, β -CH₂), 36.0 (C(CH₃)₃), 38.5 (d, ¹J_{YC} = 55.0 Hz, α -CH₂), 53.7 (C(CH₃)₃), 68.4 (α -CH₂, THF), 106.3 (ring C attached to SiMe₂), 121.7, 126.2 (ring C).

[Y(η^5 : η^1 -C₅Me₄SiMe₂NCMe₃)(μ -CH₂CH₂^{*n*}Bu)(THF-*d*₈)] (8a). In an NMR tube the *n*-hexyl complex **4a** was dissolved in THF-*d*₈. ¹H NMR (THF-*d*₈, 25 °C): δ -0.68 (br m, 2 H, α -CH₂), 0.36 (s, 6 H, SiCH₃), 0.85 (t, ³J_{HH} = 7.2 Hz, 3 H, ζ -CH₃), 1.12 (m, 2 H, ϵ -CH₂), 1.21 (s, 11 H, C(CH₃)₃ + δ -CH₂), 1.26 (m, 2 H, γ -CH₂), 1.41 (m, 2 H, β -CH₂), 1.99, 2.06 (s, 2 \times 6 H, C₅Me₄). ¹³C{¹H} NMR (THF-*d*₈, 25 °C): δ 8.8 (¹J_{CH} = 116.8 Hz, SiCH₃), 11.5, 14.4 (¹J_{CH} = 124.6 Hz, ring CH₃), 14.7 (¹J_{CH} = 123.8 Hz, ζ -CH₃), 22.6 (¹J_{CH} = 126.4 Hz, ϵ -CH₂), 32.3 (¹J_{CH} = 121.7 Hz, δ -CH₂), 32.7 (¹J_{CH} = 123.5 Hz, γ -CH₂), 35.6 (C(CH₃)₃), 37.9 (t, ¹J_{YC} = 53.4 Hz, ¹J_{CH} = 103.7 Hz, α -CH₂), 40.1 (¹J_{CH} = 123.0 Hz, β -CH₂), 54.2 (C(CH₃)₃), 106.6 (ring C attached to SiMe₂), 120.8, 125.5 (ring C).

[Y(η^5 : η^1 -C₅Me₄SiMe₂NCMe₃)(CH₂CH₂Et)(DME)] (9a). To a solution of [Y(η^5 : η^1 -C₅Me₄SiMe₂NCMe₃)(μ -CH₂CH₂Et)]₂ (**2a**; 32 mg, 41 μ mol) in toluene (1.5 mL) was added 0.5 mL (5 mmol) of 1,2-dimethoxyethane, and the solution was stirred for 15 min at room temperature. After the volume of the solution was reduced to about 0.7 mL, the solution was layered with 5 mL of hexane. Cooling to -30 °C overnight afforded colorless crystals (18 mg, 35%). ¹H NMR (toluene-*d*₈, 25 °C):

δ -0.33 (br m, 2 H, α -CH₂), 0.57, 0.74 (s, 2 \times 3 H, SiCH₃), 1.08 (t, ³J_{HH} = 7.4 Hz, 3 H, δ -CH₃), 1.35 (s, 9 H, C(CH₃)₃), 1.47 (m, 2 H, γ -CH₂), 1.52, 1.69 (m, 2 \times 1 H, β -CH₂), 1.71, 1.96, 2.12, 2.38 (s, 4 \times 3 H, C₅Me₄), 2.30, 2.51 (d, 2 \times 2 H, ³J_{HH} = 7.4 Hz, OCH₂CH₂O), 3.04 (s, 6 H, OCH₃). ¹³C{¹H} NMR: δ 8.6, 9.0 (SiCH₃), 11.2, 11.9, 13.8, 14.8 (ring CH₃), 14.4 (δ -CH₃), 32.5 (²J_{YC} = 3.4 Hz, β -CH₂), 34.2 (γ -CH₂), 35.3 (C(CH₃)₃), 37.0 (d, ¹J_{YC} = 53.3 Hz, α -CH₂), 53.8 (C(CH₃)₃), 62.4 (OCH₃), 70.1 (OCH₂CH₂O), 106.8 (ring C attached to SiMe₂), 119.6, 121.5, 123.7, 126.3 (ring C). ²⁹Si{¹H} NMR (toluene-*d*₈, 25 °C): δ -26.2 (d, ¹J_{YSi} = 1.7 Hz). ¹H NMR (toluene-*d*₈, -70 °C): δ -0.12, -0.01 (br t, 2 \times 1 H, α -CH₂), 0.83, 1.01 (s, 2 \times 3 H, SiCH₃), 1.37 (t, ³J_{HH} = 6.8 Hz, 3 H, δ -CH₃), 1.58 (s, 9 H, C(CH₃)₃), 1.72 (m, 1 H, β -CH₂), 1.84 (m, 3 H, γ -CH₂ + OCH₂-CH₂O), 1.99 (m, 2 H, β -CH₂ + OCH₂CH₂O), 2.17, 2.37 (m, 2 \times 1 H, OCH₂CH₂O), 1.84, 2.09, 2.31, 2.62 (s, 4 \times 3 H, C₅Me₄), 2.80, 3.07 (s, 2 \times 3 H, OCH₃). Anal. Calcd for C₂₃H₄₆NO₂SiY: C, 56.89; H, 9.55; N, 2.88. Found: C, 55.64; H, 9.48; N, 3.67.

[Y(η^5 : η^1 -C₅Me₄SiMe₂NCMe₃)(CH₂CH₂^{*n*}Bu)(DME)] (10a). The dimeric alkyl **4a** (27 mg, 32 μ mol) was dissolved in a mixture of 1.5 mL of toluene and 0.3 mL (3 mmol) of 1,2-dimethoxyethane. After the solution was stirred for 15 min at room temperature, its volume was reduced to 0.7 mL and it was layered with 3 mL of hexane. The solution was cooled to -30 °C overnight to give colorless crystals (13 mg, 79%). ¹H NMR: δ -0.18 (br m, 2 H, α -CH₂), 0.73, 0.91 (s, 2 \times 3 H, SiCH₃), 1.02 (t, ³J_{HH} = 7.4 Hz, 3 H, ζ -CH₃), 1.49 (s, 9 H, C(CH₃)₃), 1.61 (m, 6 H, γ -CH₂ + δ -CH₂ + ϵ -CH₂), 1.68, 1.84 (m, 2 \times 1 H, β -CH₂), 1.79, 2.09, 2.24, 2.56 (s, 4 \times 3 H, C₅Me₄), 2.30, 2.51 (d, 2 \times 2 H, ³J_{HH} = 7.4 Hz, OCH₂CH₂O), 3.07 (s, 6 H, OCH₃). ¹³C{¹H} NMR: δ 8.6, 9.0 (SiCH₃), 11.2, 11.9, 13.8, 14.8 (ring CH₃), 14.7 (ζ -CH₃), 23.6 (ϵ -CH₂), 31.6 (δ -CH₂), 32.4 (γ -CH₂), 35.3 (C(CH₃)₃), 37.5 (d, ¹J_{YC} = 53.4 Hz, α -CH₂), 39.7 (d, ²J_{YC} = 3.0 Hz, β -CH₂), 53.8 (C(CH₃)₃), 62.4 (OCH₃), 70.1 (OCH₂CH₂O), 106.8 (ring C attached to SiMe₂), 119.6, 121.5, 123.7, 126.2 (ring C). ²⁹Si{¹H} NMR: δ -26.2 (d, ¹J_{YSi} = 1.5 Hz).

Kinetics of the Reaction of 1a with 1-Hexene. A 5 mm NMR tube with a Teflon valve was charged with **1a** (19 mg, 23 μ mol) and a mixture of C₆D₆ (750 μ L) and THF (20 μ L, 247 μ mol). After addition of 1-hexene (75 μ L, 606 μ mol), the sample was inserted into the thermostated probe (\pm 0.5 °C) of the spectrometer and an initial ¹H NMR spectrum ($t = 0$) was recorded. The integral of the YHY protons was monitored as a function of time (8 scans were recorded every 6 min 37 s over a period of 3 h at 25, 27, 30, 32, and 35 °C); the integral *I* of the YHY group was determined relative to the area of the integral of the residual undeuterated solvent as an internal standard. The data were fit by linear least-squares analysis to a first-order rate expression. The plot of ln(*I*₀/*I*) vs *t* with *I*₀ = *I* ($t = 0$ s) afforded *k* from the slope *a*. The rate constants obtained at different temperatures were fit to the Eyring equation by linear least-squares analysis. ΔH^\ddagger and ΔS^\ddagger were obtained from the slope and the axial section ($\Delta H^\ddagger = 26 \pm 2$ kcal mol⁻¹ and $\Delta S^\ddagger = 11 \pm 1$ cal K⁻¹ mol⁻¹).

Crystal Structure Analysis of 2a, 2b, 3b, 4a, 6a, and 9a. Relevant crystallographic data for **2a**, **2b**, **3b**, **4a**, **6a**, and **9a** are summarized in Tables 1 and 3. Single crystals suitable for X-ray crystal structure analysis were obtained by cooling concentrated toluene solutions of **2a**, **2b**, **3b**, **4a**, and **9a** to -30 °C or from a concentrated benzene/hexane (1:10) solution of **6a** at room temperature. Data collections for **2b**, **3b**, **4a**, and **6a** were performed using ω scans on an Enraf-Nonius CAD-4 diffractometer with graphite-monochromated Mo K α radiation at 296(2) K. Data collection for Lorentz-polarization and absorption (empirically using ψ scans) was carried out using the program system WinGX.^{38a} For **2a** and **9a** the data collection was carried out with a Bruker AXS diffractometer, and the data collection as well as the data reduction and correction for absorption was carried out using the program system SMART.^{38b} The structures were solved by Patterson

and difference Fourier synthesis (SHELXS-86).^{38c} From the measured reflections, all independent reflections were used, and the parameters were refined by full-matrix least squares against all F_o^2 data (SHELXL-97)^{38d} and refined with anisotropic thermal parameters. All hydrogen atoms in **3b**, **4a**, and **6a** were included in calculated positions; in **2b** and **9a**, they could partly be refined in their positions. In **2a**, all hydrogens

were found and refined in their positions with isotropic thermal parameters.

Acknowledgment. Generous financial support by the Deutsche Forschungsgemeinschaft and the Fonds der Chemischen Industrie is gratefully acknowledged. We thank Dr. B. Mathiasch and Dr. N. Rees for obtaining various NMR spectroscopic data and S. Hennig for collecting the diffraction data of **2a** and **9a**.

Supporting Information Available: Tables of all crystal data and refinement parameters, atomic parameters including hydrogen atoms, thermal parameters, and bond lengths and angles for **2a**, **2b**, **3b**, **4a**, **6a**, and **9a**. This material is available free of charge via the Internet at <http://pubs.acs.org>.

OM0206599

(38) (a) Farrugia, L. J. WinGX-Version 1.64.02, An Integrated System of Windows Programs for the Solution, Refinement and Analysis of Single Crystal X-ray Diffraction Data. *J. Appl. Crystallogr.* **1999**, *32*, 837. (b) ASTRO, SAINT and SADABS. Data Collection and Processing Software for the SMART System; Siemens Analytical X-ray Instruments Inc., Madison, WI, 1996. (c) Sheldrick, G. M. SHELXS-86, Program for Crystal Structure Solution; University of Göttingen, Göttingen, Germany, 1986. (d) Sheldrick, G. M. SHELXL-97, Program for Crystal Structure Refinement; University of Göttingen, Göttingen, Germany, 1997.